ELM control strategies and tools: status and potential for ITER

P.T. Lang, A. Loarte 1), G. Saibene 2), L.R. Baylor 3), M. Becoulet 4), M. Cavinato 2), S. Clement-Lorenzo 2), E. Daly 1), T. E. Evans 5), M. E. Fenstermacher 6), Y. Gribov 1), L. D. Horton 7), C. Lowry 7), Y. Martin 8), O. Neubauer 9), N. Oyama 10), M. J. Schaffer 5), D. Stork 11), W. Suttrop, P. Thomas 2), M. Tran 8), H. R. Wilson 12), A. Kavin 13)

IPP Tokamak Scenario Development Division, MPI für Plasmaphysik,
EURATOM Association, Boltzmannstr. 2, 85748 Garching, Germany
1) ITER Organization, Route de Vinon sur Verdon, 13115 St Paul Lez Durance - France
2) F4E Joint Undertaking, Josep Pl. 2, Torres Diagonal Litoral B3, 08019, Barcelona, Spain
3) Oak Ridge National Laboratory, Box 2008, Oak Ridge, TN 37831, USA
4) CEA, IRFM, F-13108, Saint-Paul-lez-Durance, France
5) General Atomics, PO Box 85608, San Diego, CA 92186-5608, USA
6) Lawrence Livermore National Laboratory, PO Box 808, Livermore, CA 94550, USA
7) JET-EFDA, Culham Science Centre, Abingdon, OX14 3DB, UK
8) EPFL, 1015 Lausanne, Switzerland
9) Forschungszentrum Jülich, Institute of Energy Research, D-52425, Jülich, Germany
10) Japan Atomic Energy Agency, Naka Fusion Institute, Naka, 311-0193, Japan
11) CCFE, Culham Science Centre, Abingdon, Oxon, OX14 3DB, UK
12) University of York, Department of Physics, York, YO10 5DD, UK
13) Efremov Institute, St Petersburg, Russia

E-mail contact of author: peter.lang@aug.ipp.mpg.de

Short tile: ELM actuation status and ITER perspectives

Abstract

Operating ITER in the reference inductive scenario at the design values of I_P = 15 MA and Q_{DT} = 10 requires the achievement of good H-mode confinement that relies on the presence of an edge transport barrier whose pedestal pressure height is key to plasma performance. Strong gradients occur at the edge in such conditions that can drive MHD instabilities resulting in Edge Localized Modes (ELMs), which produce a rapid energy loss from the pedestal region to the plasma facing components. Without appropriate control, the heat loads on plasma facing components during ELMs in ITER are expected to become significant for operation in H-mode at I_P = 6 - 9 MA; operation at higher plasma currents would result in a very reduced life time of the plasma facing components.
Currently, several options are being considered for the achievement of the required level of ELM control in ITER; this includes operation in plasma regimes which naturally have no or very small ELMs, decreasing the ELM energy loss by increasing their frequency by a factor of up to 30 and avoidance of ELMs by actively controlling the edge with magnetic perturbations. Small/no ELM regimes obtained by influencing the edge stability (by plasma shaping, rotational shear control, etc.) have shown in present experiments a significant reduction of the ELM heat fluxes compared to type-I ELMs. However, so far they have only been observed under a limited range of pedestal conditions depending on each specific device and their extrapolation to ITER remains uncertain. ELM control by increasing their frequency relies on the controlled triggering of the edge instability leading to the ELM. This has been

presently demonstrated with the injection of pellets and with plasma vertical movements; pellets having provided the results more promising for application in ITER conditions. ELM avoidance/suppression takes advantage of the fact that relatively small changes in the pedestal plasma and magnetic field parameters seem to have a large stabilizing effect on large ELMs. Application of edge magnetic field perturbation with non-axisymmetric fields is found to affect transport at the plasma edge and thus prevent the uncontrolled rise of the plasma pressure gradients and the occurrence of type-I ELMs. This paper compiles a brief overview of various ELM control approaches, summarizes their present achievements and briefly discusses the open issues regarding their application in ITER.

1. Introduction

The main goal of current research in the field of magnetically confined plasmas aiming for power generation by nuclear fusion is to optimize high confinement plasma regimes (H-mode) in order to achieve the maximum plasma energy for a given input heating power P_{in}. Thus, in future fusion devices such as the ITER tokamak, which is expected to produce considerable amounts of fusion power P_{fus}, the gain or amplification factor $Q = P_{fus}/P_{in}$ requires to be maximized as well. High confinement H-mode plasmas are characterized by the existence of an Edge Transport Barrier (ETB) in a narrow edge region inside the last closed flux surface (separatrix). Inside this ETB the ion transport is reduced to values similar to those predicted by neoclassical transport and a steep gradient builds up in both the temperature and the density profiles. As a consequence, both profiles rise steeply inside the separatrix, which leads also to their increase in the plasma core, with the resulting profiles looking similar to those obtained in the low confinement L-mode (observed for input power below a certain L-> H threshold) but displaced upwards by a pedestal. This is shown in Figure 1 displaying typical resulting radial pressure profiles for L-mode and H-mode confinement. It is well established, both experimentally and theoretically, that in standard H-mode scenarios, the steep pressure gradient in ETBs is limited by Magneto Hydro Dynamic (MHD) instabilities called Edge Localized Modes (ELMs) [1, 2]. The dynamics of a spontaneously occurring type-I ELM consists of several different phases. A precursor phase is followed by a linear growth phase of the instability that finally evolves into a non-linear MHD phase which leads to the temporary break down of the transport barrier resulting in a loss of pressure and current from the pedestal plasma region. Between ELMs (or recovery phase) the edge pressure and current are recovered by the continuous outflow of plasma energy and particles in the re-established ETB and continue to build up until the stability boundary is reached again leading to the next ELM. Hence, in this operational regime the edge pedestal undergoes a limit cycle oscillation causing a periodic collapse of the pedestal plasma leading to intermittent energy and particle pulses from the confined plasma onto plasma facing components. Analysis of experimental measurements in tokamaks indicates that a significant amount of the energy lost by the plasma during ELMs reaches the plasma facing components (PFCs) in toroidally and polodailly localised areas such as the divertor target [3]. As the plasma energy is expelled by the ELMs in very short timescales (~100s μs), the local power fluxes caused by the ELMs are expected to be significant and cause local overheating of the plasma facing components, a problem whose seriousness is expected to increase with the size of the tokamak.. Whereas for mid-size tokamaks (minor radius a_0 about 0.5 m) ELMs are not found to cause any damage to plasma facing components, the larger sized JET (a_0 about 1.0 m) observed already melting of the Be divertor surfaces and large impurity influxes caused by loosely attached hydrocarbon layers affecting the plasma performance for the largest ELMs [4]. In ITER, uncontrolled type-I ELMs are thus expected to cause significant impurity influxes into the main plasma and shorten the lifetime of plasma facing component including by evaporation and melting during these events.

The ITER Q ~ 10 scenario is based on the type-I ELMy H-mode regime, which has a very broad experimental and theoretical basis (see [5] and references therein). Unmitigated type-I ELMs in this scenario could correspond to losses of up to 20% of the pedestal plasma energy resulting in ~ 20MJ energy loss per ELM (ΔW_{ELM}) [6]. On the basis of experimental data [7] and the expected pedestal plasma parameters in ITER, the temporal structure of the ELM energy pulse at the divertor [8] and the detailed spatial structure of the energy flux at the castellated structures during an ELM [9] have been evaluated. This leads to a requirement of a maximum ELM energy flux of 0.5 MJm^{-2} for 15 MA Q ~10 operation that can be deposited repetitively at the ITER divertor without a major reduction of the divertor lifetime [10]. For energy fluxes within this limit melting of the W divertor target in ITER is avoided at all locations (i.e., including castellations' edges) but significant cracking of the W surface may occur. Exceeding this value by a factor of 2-3 would cause localised melting and erosion over small areas of the target and to significant W impurity influxes into the core plasma. Both of these have undesirable consequences for ITER operation if repeated at the rate (few Hz) expected for uncontrolled ELMs in ITER (i.e. 500-1000 ELMs per Q~10 discharge): in the first place large W influxes caused by the ELMs could lead to increased disruptivity of ITER plasmas by W accumulation and radiative collapse. Even if this is avoided, the localised removal of as little as 0.1 μm of W divertor material per ELM would limit the divertor lifetime to less than a hundred Q ~ 10 discharges, thus decreasing significantly the experimental availability of the ITER device. Type-I ELM mitigation and/or avoidance techniques must be thus available in ITER to maintain the energy fluxes to plasma facing components under the required maximum value thus ensuring that melting by ELM events is routinely avoided and that the erosion lifetime of the plasma facing components is appropriate for an efficient scientific exploitation of ITER as an experimental facility.

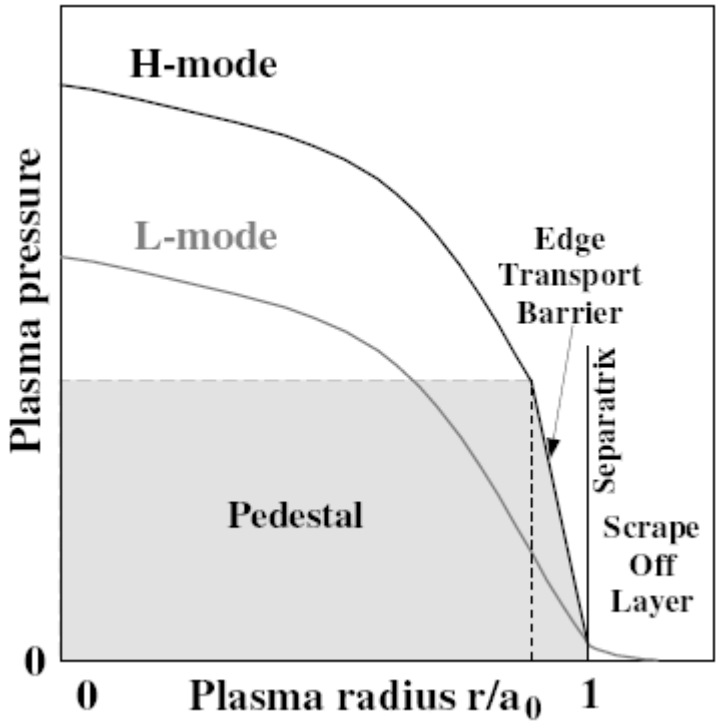

Figure 1: Typical pressure profiles observed in L- and H-mode phases. Establishing a transport barrier just inside the last closed flux surface creates a strong gradient at the edge adding a pedestal to the L-mode profile during H-mode phases.

The requirement for the acceptable maximum energy density during controlled ELMs of 0.5 MJm^{-2} for 15 MA Q~10 plasmas can be transformed into a limit for the maximum energy lost from the main plasma during controlled ELMs in these conditions. Assuming an asymmetry of 2:1 for energy deposition at the inner versus the outer divertor and that the area for ELM energy deposition is the same as that for stationary power flux for attached divertor (both of which assumptions are known to be conservative) controlled ELM operation requires a maximum energy lost by the plasma during the ELM of ΔW_{ELM} = 0.66 MJ [8]. The ratio of the ELM energy losses expected for spontaneous uncontrolled ELMs in the Q = 10 scenario to the maximum value for controlled ELMs (required to avoid divertor erosion) is ~ 30 (20 MJ/0.66 MJ), this quantifies the requirement for reduction of the ELM size in ITER. Recent experimental evidence from JET [11] has shown that the area for energy deposition at the divertor is dependent on the ELM energy loss itself and increases with ΔW_{ELM}, with very small areas for ELM deposition (compared to those between ELMs) for small ELMs. While this decreases the expected divertor loads by ELMs for uncontrolled ELMs and can expand somewhat the operational space at low currents, it also weakens the effect of an increasing ELM frequency on reducing the peak divertor ELM heat load so that the required frequency enhancement/reduction of ΔW_{ELM} for 15 MA operation with Q = 10 remains at a level of 30 even when this effect is considered [8]. On the basis of the considerations above, it is expected and foreseen in the ITER Research Plan that control of ELMs will be not only required for full performance operation at 15 MA Q ~ 10 but also over a significant part of its operational space in the H-mode regime where I_p > 6-9 MA [8]. Therefore, it is foreseen to install and develop ELM control schemes and control strategies during the non-active phase of ITER operation in which low current H-mode operation will be performed for the first time, most likely with Helium plasmas [10]. For the development and control of higher current H-mode scenarios in ITER, it is found advantageous to enter the H-mode regime before the current reaches the flat top and to maintain it during the ramp-down phase. As the current level during these phases could exceed the range in which uncontrolled ELMs could cause significant erosion of the divertor, ELM control during these phases with a varying plasma current and edge safety factor is also required..

Many experiments at different tokamak devices have been dedicated to the investigation of the problem of ELM control with a view to provide solutions which are applicable to ITER by the application of different approaches. In this paper a brief overview of the different ELM control techniques investigated and their potential application to ITER is given. Section 2 describes the basic physics guidelines on which ELM control schemes are based. Sections 3-7 describes the various approaches that can be followed for ELM control, providing a short overview of the achievements made and the status of development reached followed by the pros and cons of every technique as well as the outstanding R&D issues that remain to be addressed in each area for a successful application in ITER. For the latter aspects, we will refer in this paper to the main outcome of the assessments carried out by the ITER Organization and the European Union Domestic Agency Fusion for Energy (F4E) whose details can be found in [10, 12].

2. ELM control strategies

Any successful control strategy needs to identify possible parameters on which control can be performed. For control purposes, an appropriate description of the operational boundaries for the H-mode pedestal is provided by the calculated ideal MHD limit for coupled peeling-ballooning modes [12], which can describe the maximum achievable pedestal pressure in the experiments as well as its increase with plasma shaping. In this description the boundary of pedestal parameters for which an ELM instability would occur is evaluated by calculating the stability constraints on the pedestal for coupled peeling-ballooning modes driven by both the pressure edge gradient and, a consequence of the sharp pressure gradients, the large bootstrap

current in the pedestal region. A schematic stability diagram produced by such approach (for further details see [13]) is shown in Figure 2. Ballooning modes with toroidal mode numbers n in the range of about 6-10 are most unstable at high pedestal pressure gradient (p'_{ped}) and low parallel current (I_{ped}). At high I_{ped} and low p'_{ped} peeling modes are the limiting instabilities. In the region of both high p'_{ped} and I_{ped} coupled peeling-ballooning modes are found to be the limit for edge MHD stable operation. Due to the strong coupling between core and pedestal in high confinement regimes, a high pedestal pressure is required for high confinement and thus a high p'_{ped}. For low collisionality conditions high p'_{ped} unavoidably implies the generation of a large bootstrap current at the edge so that, for high confinement regimes, the expected MHD stability limit is determined by coupled peeling-ballooning modes. The stability boundary for the pedestal depends strongly on the plasma shape, so that the edge stability domain can be extended, for example, by increasing the triangularity allowing the access to higher I_{ped} and p'_{ped}.

A sketch of the typical evolution during a type-I ELM is shown also in Figure 2. After the ELM collapse, or once the ETB is re-established, the edge pedestal starts growing. The pressure gradient increases on a transport time scale and the associated bootstrap current evolves accordingly. It is usually observed that the pedestal gradient recovers rather quickly after the ELM crash and then gradually increases slowly towards its maximum value. This behaviour is attributed to the closeness to a ballooning limit which in some cases comes associated with growing fluctuations indicating the linear growth of edge MHD during the so-called precursor phase [14]. In many cases the plasma can remain near the maximum pressure limit for several ten milliseconds while in other cases the ELM is triggered immediately after the recovery of the pressure profile [15]. In either case, when the edge pressure gradients and edge currents are such that the plasma approaches the limit in the peeling-ballooning corner of the stability domain, a sudden collapse of the edge plasma caused by the nonlinear MHD expulsion of plasma filaments which is predicted to occur close to the values for which the linear stability threshold is exceeded [16]. During this collapse phase the expulsion of particles and energy from the edge plasma occurs which when, interacting with the plasma facing components, can lead to the problems discussed in the introduction.

In view of the hard and sudden nature of the ELM instability triggered at the peeling-ballooning boundary, any reasonable ELM control strategy should be based on avoiding the plasma reaching this maximum limit either by limiting the pressure gradients and edge currents at values which are stable or by causing a controlled ELM-like crash which releases a much smaller amount of energy from the plasma than that when the plasma reaches the maximum limit. In addition, it is possible that some of the energy released by the plasma can be lost by radiation before it is deposited at the plasma facing components. Estimates for ITER [17] show that this effect can indeed be significant for very small ELM energy losses but becomes small for the energy losses expected during uncontrolled ELMs in ITER and cannot thus be relied solely as a solution to the control of ELM power fluxes in ITER.

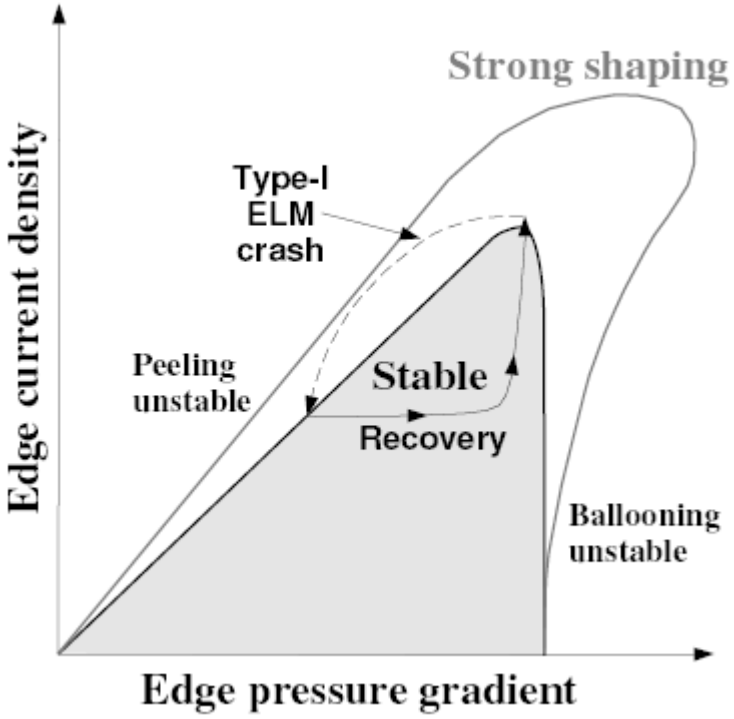

Figure 2: Schematic view of the edge stability boundaries showing the variation of pedestal boundaries with discharge shaping, limiting instabilities and model of the type-I ELM cycle.

Therefore, we will consider in this paper the two following ELM control strategies and discuss their potential for achieving the required level of ELM control in ITER:

a) The most obvious but also more challenging ELM control strategy is based on maintaining the edge plasma conditions so that the edge pressure is high enough, ensuring the required core plasma performance, but at the same time it stays away from the stability limit that leads to the triggering of type-I ELMs. These schemes envisage controlling the edge plasma parameters so that the edge pressure gradient/edge current are maintained high and very close to the stability limit while avoiding reaching it in a controlled way. This can be achieved by increasing the level of transport in the ETB so that the plasma pressure and pressure gradient saturates to a lower value than that required for the triggering of type-I ELMs. Examples of this scheme are the control of ELMs by the application of external magnetic perturbations and the same process can occur naturally in the plasma in some conditions for the small/no ELM regimes discussed in the next section.

b) The other basic way of ELM control consists on de-stabilizing the plasma to trigger an ELM before the maximum stability limit is reached. This is achieved by introducing a perturbation in the plasma so that the instability is triggered at lower pressures than the maximum limit which leads to a smaller ELM energy loss. In this approach the ELMs are triggered at will at a suitable frequency and, for this reason, such techniques are generally known as ELM pacing. The ELM pacing techniques, such as pellet injection, and fast vertical plasma motion rely on the observed inverse dependence of ΔW_{ELM} on the ELM frequency f_{ELM}. The empirical relation $\frac{\Delta W_{ELM} \times f_{ELM}}{W} \times \tau_E = \frac{\Delta W_{ELM} \times f_{ELM}}{P} = 0.2 - 0.4$ found for type-I ELMs in a wide range of plasma parameters and different devices for spontaneous [18] but also for paced ELMs without deterioration of the plasma performance [19] show the

possibility to decrease the ELM energy loss by increasing their frequency in a controlled way.

In the following sections we will describe the various possibilities pursued in present experiments to achieve the required level of ELM control in ITER following the two approaches above and their potential for application in ITER as well as the open R&D issues. In the first place we will discuss the possibility of achieving this required level by appropriate choice of plasma operational regime, the so-called small/no ELM regimes which may not require, as such, active schemes to act on the pedestal plasma to eliminate or decrease the ELM size to an acceptable level in ITER. We will then proceed to analyse other possible ELM control schemes which require specially conceived actuators to achieve the required effect on the pedestal plasma and/or ELMs energy loss.

3. Small/no ELM regimes

Small/no ELM regimes in tokamaks have been widely investigated in order to develop a scenario that avoids large type-I ELMs typical of high confinement H-modes while, at the same time, maintaining a similar level of energy confinement to them. The investigations have centered on achieving these favorable pedestal ELM conditions by tuning the operational regimes in the tokamaks such as by plasma shaping, plasma rotation, adding extrinsic impurity radiators, etc. An exhaustive overview of all the multifaceted aspects of the experimental results obtained is beyond the scope of this paper; here we only describe them in view of their potential application as scenarios with acceptable ELMs in the operation of ITER.

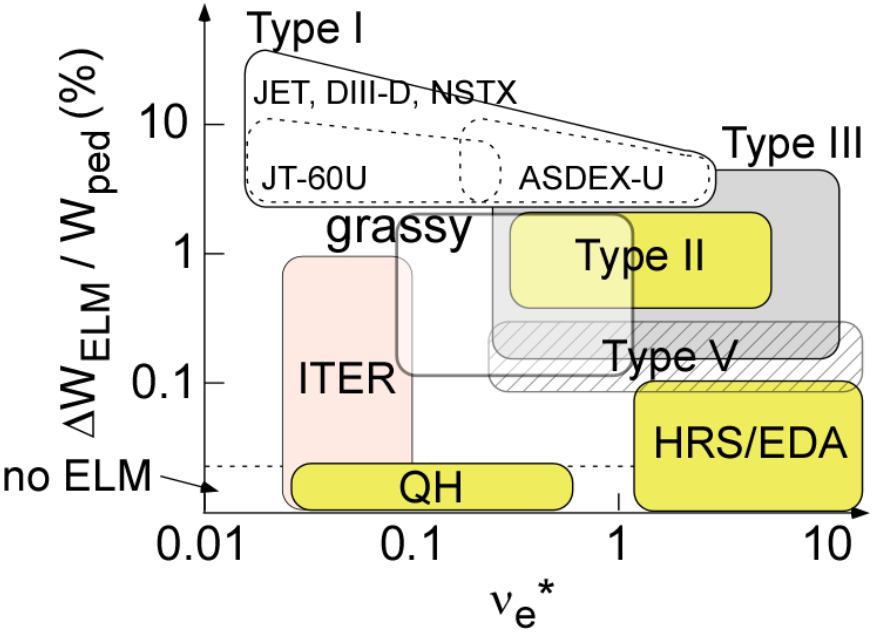

Figure 3: Comparison of operational space in normalized ELM energy loss and edge collisionality. Regimes marked by a yellow shade indicate edge fluctuations seem to play an important role in ELM mitigation [20].

Small/no ELM regimes can be widely categorized by their pedestal conditions in terms of the operational space in non-dimensional pedestal parameters and requirements of plasma shape and configuration [20]. An overview of the experimental plasma conditions for which such regimes are obtained is given in Figure 3 [21]. Figure 3 shows the operational space achieved for several regimes with small ELMs or no ELMs in terms of the normalized ELM energy loss versus edge collisionality. In many of these regimes there is enhanced edge

turbulence/MHD activity which affects edge transport and is correlated with the existence of the small/no ELMs regime itself. A more detailed description of these regimes, typical parameter regimes established in different devices and the characteristics of edge fluctuations and MHD activities can be found e.g. in [20].

EDA and HRS regime

As shown in Figure 3, both the Enhanced Dα (EDA) and the High Recycling Stationary (HRS) regime show considerable reduction of the ELM size and the heat load onto the divertor plates in contrast to the type-I ELMy H-mode regime. The EDA plasmas found in Alcator C-Mod are characterised by the occurrence of an edge fluctuation that increases significantly the perpendicular particle transport. This quasi-coherent mode (QCM) shows a strong in/out asymmetry with the largest amplitude being localised at the outer mid plane. Its maximum amplitude is found just inside the separatrix with aradial width leading to a non-zero amplitude outside the separatrix which is qualitatively consistent with the measured particle transport enhancement [22]. A very similar behaviour is reported for the High Recycling Steady (HRS) high confinement regime in the JFT-2M tokamak for which stationary pedestal conditions in the absence of the large ELMs are achieved with coherent magnetic fluctuations in the frequency range of the order of 10–100 kHz [23]. Observations both in Alcator C-Mod and JFT-2M are thus consistent with the need to create conditions for which a mode appears in the plasma edge which leads to an increased transport across the edge transport barrier that replaces the energy and particle out flux from the plasma by ELMs by much smaller turbulent events at very high frequency. It is important to note that for these conditions the pedestal collisionality is high and, thus, the level of bootstrap current is expected to be very low so that the edge plasma would not be unstable to peeling modes under any value of edge pressure gradient. [24]. In fact, it is this need for high collisionality for the required edge high frequency modes in this regime to appear and suppress the ELMs and the consequent low edge bootstrap current which makes their extrapolability to ITER very uncertain. ITER operation in scenarios with high fusion gain are expected to require high edge pedestal pressure and temperature so that the edge collisionality will be very low and the edge bootstrap current consequently high ($\nu^* < 0.05$) [10].

Grassy ELMs

Small size "grassy" ELMs appearing in a lower collisionality regime have been achieved in JT-60U demonstrating full non-inductive operation without pedestal pressure degradation. To enter the regime, several important parameters have been found such as high safety factor, high shaping (triangularity ~0.6) and high poloidal beta (β_p) [25]. Also the toroidal rotation frequency has been found to influence strongly ELM frequency and size. In case of high counter rotation, ELM frequencies in the kHz range are observed with the ELM loss size ΔW_{ELM} even dropping below the detection limit of the diamagnetic loop measurement of about 10 kJ [26]. The regime was reproduced at ASDEX Upgrade [27] and JET confirming importance of q_{95}, δ and β_p. JET also identified some requirements which seem to be common to both devices to achieve this regime besides those of q_{95}/δ; namely the need for $\beta_p > 1.6$ and $l_i > 1.0$ for discharges with strong plasma co-rotation [28]. For discharges with lower values of co-rotation or counter rotation, lower values of β_p are compatible with this regime in JT-60U (although $\beta_p \sim 1$ even in these cases) [21]. These requirements make this regime unlikely for application to full performance $Q_{DT} = 10$ ITER operation at maximum current, which requires $q_{95} \sim 3$ and $\beta_p \sim 0.65$. For lower current/long pulse advanced scenarios based on hybrid/shear optimised regimes with high normalised confinement, the requirements in terms of q_{95} and β_p to achieve the grassy ELM regime are compatible with the performance requirements and, thus, grassy ELMs could be an option for ELM control in these scenarios. The major extrapolability issue in this case concerns the experimental requirement of

relatively peaked current profiles to achieve the grassy ELMs as this would be incompatible with the expected plasma current profile shape required to achieve advanced scenario in ITER.

Type-III ELMy H-mode

The type-III regime is a very well established small ELM regime observed in many tokamaks. The type-III ELMy H-mode occurs at power levels marginally above the H-mode threshold (for discharges with favourable ion ∇B-drift direction for H-mode access). Type-III ELMs have usually a very high frequency and very small energy losses and their frequency decreases with increasing heating power. Stationary operation with type-III ELMs is usually found also to impose an upper limit on the pedestal temperature under the values that are reached by the type-I ELMy H-mode and is thus restricted to reduced plasma performance [29]. The type-III ELMy H-mode regime has been extended to higher levels of additional heating by increasing the edge density and/or by increasing the radiated power with injection of extrinsic impurities, Injection of impurities allows achieving the type-III ELMy H-mode regime at lower collisionalities than by increasing the edge density and the extrapolated ELM size in these conditions are suitable to meet the requirements for ITER Q = 10 operation [30], as it will be discussed in more detail later in this section. The major outstanding issue, however, is that the type-III ELMy H-mode comes associated with a reduced pedestal pressure so that the energy confinement experimentally achieved in this regime is substantially deteriorated with respect to this of a type-I ELMy H-mode, with typical normalised confinement in the range H_{98} = 0.65-0.85 in both JET [30] and JT-60U [31]. This implies a fusion performance of $Q \leq 5$ for ITER at a current level of 15 MA, and thus insufficient to meet the ITER Q = 10 expected at this level of current.

Type-II & Type-V ELMs

Type-II ELMs are typically observed in ASDEX Upgrade and JET for strongly shaped (high δ) plasmas in a quasi-double null configurations with a typical proximity between the separatrix and the flux surface to the upper X-points at the midplane of about 1 cm and moderately high q_{95} = 3.5-4.5 [32]. These ELMs are observed at high densities and cause deterioration of the confinement, however this can be mitigated by combining this regime with a high β_N hybrid-like regime. Key major issues still remain to be addressed for the regime regarding the viability of operation in ITER in such regime. Observations indicate that the regime can only be observed for sufficiently low pedestal temperature or high pedestal collisionality [32] unlikely to be met in ITER. The need for quasi-double null operation imposes operational requirements which may be difficult to meet in ITER because of the associated plasma position control and the power handling limitations of the ITER first wall in the vicinity of the upper X-point. Finally $q_{95} \sim 4$ operation in ITER implies operation at a plasma current level of ~ 11 MA which is incompatible with the achievement of Q = 10 for the standard H-mode confinement level [10].

Type-V ELMs have been reported from NSTX [33] for single null configurations. In this regime, larger gaps between the separatrix and the flux tube through the second X-point seem to be advantageous. For high triangularity shapes, pulling the upper X-point upward in a balanced double null configuration towards a dominant lower single null is found to change the ELM characteristics from type-I to type-V [34]. Type-V ELMs, individually, have no measurable impact on the stored energy. They show clear short-lived electromagnetic n = 1 precursors rotating in the counter current direction and filaments drifting radially outwards while propagating counter current as well. Different to type-I ELMs, in type-V ELMs single filaments were observed along open field lines far outside the separatrix and even beyond the second X-point. The regime shows thus features favourable for ITER. However, its observation is restricted to one device and the underlying instabilities responsible for the onset

of type-V ELMs have not been characterised to a level in which a meaningful extrapolation to ITER can be considered at this stage.

QH-mode

The quiescent H (QH) - mode shows, as indicated by the name attributed to this regime, a smooth evolution of the pedestal region avoiding large transient energy losses caused by the type-I ELMs. This regime shows confinement levels similar to those of the baseline type-I ELMy H-mode and was first observed in DIII-D [35] and then reproduced in other tokamaks such as AUG [36], JT-60U [37] and JET [38]. Typical operational features to achieve this regime are plasma shapes with a large clearance between the separatrix and all first wall components and counter current NBI heating. The latter is not a necessary criterion since QH-mode operation has also been demonstrated with zero momentum input [39] and also with NBI injection in co current direction [40]. Like in the EDA and HRS regimes, an edge mode (EHO or edge harmonic oscillation) is found to be present near the separatrix during QH-modes and to provide an enhanced particle out flux from the core plasma thus avoiding the uncontrolled density/pressure rise that ends up in the type-I ELMs. Recent observations from DIII-D [39] have shown that the shear in the edge rotation is an important parameter to achieve and maintain the QH-mode. This is in line with linear edge MHD stability analysis that shows that the QH mode edge plasma is situated near the current limited stability boundary at high edge current density and large pressure gradient [41] so that the EHO could correspond to a saturated peeling mode stabilized by rotational shear. Given the limited capability for momentum input in ITER, the achievement of a significant edge rotational shear implies the application of non-resonant edge magnetic perturbations which lead to an effective torque being applied to the edge plasma and thus to increased rotational shear. The application of such a scheme in ITER would most likely require a system of in-vessel coils to ensure that the magnetic field perturbation in the central part of the plasma is maintained as low as possible in order to minimize the effect on core plasma rotation. Further analysis is required to determine if this is the case or an external coil system would also be appropriate to achieve the required edge rotational shear while maintaining an appropriate core plasma rotation [10]. Another important issue for the applicability of this regime is its compatibility with the required core plasma and separatrix density in ITER. The expected density at which the plasma would be in a similar stability condition as in DIII-D depends on the model assumed for the pedestal and goes from a factor of 2 lower than the ITER reference operating density for Q=10 in the initial estimates [42] to values similar or even higher than those foreseen for ITER for predictions with an improved model for the pedestal width physics [43]. If the latter results are confirmed and it can be demonstrated that it would be feasible in ITER to achieve the required level of edge rotational shear, the QH-mode regime would be a very attractive operational mode to achieve Q = 10 in ITER in a regime without type-I ELMs. Further R&D is needed and is in progress along these lines to confirm these two key issues before the QH-mode can be put forward as an alternative regime to the controlled type-I ELMy H-mode for the achievement of Q=10 in ITER.

Radiative scenarios

To conclude this section we describe in more detail the radiative scenarios as a particular subset of the type-III ELMy H-mode regime, although we also discuss some results obtained in the type-I ELMy H-mode. A number of experiments have been carried out to replace the intrinsic carbon (C) radiation by an extrinsic radiator which becomes critical for sustained high power operation in all metal machines such as ASDEX Upgrade, Alcator C-Mod and, recently, JET with a Be wall and a W divertor.

Nitrogen seeding in the standard inductive scenario and also in the high beta hybrid scenario considered for long pulse operation in ITER has been applied to establish highly radiative

type-III ELMy H-mode conditions at JET [30]. It these experiments it was found that the average divertor power load was significantly reduced by the nitrogen seeding, achieving radiative power fractions up to 97 %. Most of the power was radiated in the divertor and X-point region outside $r = 0.9\ a_0$, just on top and outside the pedestal. In this case, some of the already rather small type-III ELM energy loss is dissipated by radiative process at the plasma edge before it reaches the PFCs. On the contrary, when the radiative H-modes are maintained in the type-I ELMy H-mode regimes no significant radiative dissipation of the ELM energy flux takes place [44, 45]. The main issue regarding the application of this regime to ITER concerns the degraded pedestal pressure and core plasma confinement which is associated with the type-III ELMy H-mode. Scaling of the JET results would require ITER operation at 17 MA to achieve Q = 10 [44, 30], which poses significant issues related to disruptions at these very large current levels. Another approach to the ELM control in radiative plasmas has been developed by the integrated exhaust control (IEC) scenario at ASDEX Upgrade, which aims to control simultaneously the power flux during an ELM but also between ELMs together with the particle removal rate [46]. In addition, since ASDEX Upgrade has W plasma facing components, an acceptable low W concentration had to be kept in this scenario. The actuators used in these experiments were valves controlling deuterium fueling and argon (Ar) radiating gas feedback controlled on the neutral divertor flux and the divertor temperature (thermoelectric currents measured by shunts). For plasma operating in the type-I ELMy H-mode regime, no confinement reduction but even an improvement of particle confinement resulting from a rise in the electron density in the core plasma results when the adding nitrogen seeding and, in fact, the performance of improved H-mode discharges can increase by up to 25% in these radiative regimes [47]. In these conditions, pellet pacing was utilized to maintain a minimum ELM frequency and ELM divertor power fluxes were substantially reduced with evidence of significant mitigation due to re-radiation of the plasma energy [48], an effect, which, as mentioned above, may only be restricted to small ELM losses in ITER [17]. On the other hand, when these regimes where explored in the type-III ELMy H-mode regime a significant confinement degradation similar to that observed at JET [30,44] was also found in ASDEX Upgrade raising the issues discussed above regarding the applicability of this regime for high Q operation in ITER.

Suitability of small/no ELM regimes to achieve ITER objectives

From the discussions above, it is clear that some of the features of the small ELM/no ELM regimes are very interesting for their application in ITER. However, in all cases there are significant compatibility issues between the experimental requirements in these plasma regimes (high collisionality, closeness to double null, control of edge rotational shear, etc.) and those needed to achieve the required plasma performance in ITER beyond those of ELM control, such as appropriate level of core confinement, acceptable stationary power flux control to PFCs, sufficient plasma rotation to avoid confinement deterioration and increased disruptivity, etc. In view of this, there is no sufficient evidence at this stage to change the basis for the evaluation of the plasma operation and performance in ITER from the type-I ELMy H-mode and, thus, active ELM control methods for plasmas in this regime should be considered. On the other hand, it is important that R&D in the small/no ELM regimes experiments is continued in present tokamaks to determine whether the ITER compatibility issues described above can be circumvented and/or to develop a firmer physics basis for the extrapolation of this regimes to ITER that can demonstrate that the regimes will be compatible with the other requirements for successful operation at the ITER scale.

4. Edge magnetic perturbations

Application of perturbations to the edge magnetic field in tokamaks has been seen to affect ELM behaviour in many devices. This scheme has demonstrated its potential by either

reducing drastically or eliminating completely the ELM power fluxes onto plasma facing components and substituting it by an approximately constant power out flux. The initial physics basis for this scheme of ELM suppression postulated that radial plasma transport could be enhanced in the pedestal region by the creation of an ergodic layer thus controlling the rise of the pedestal pressure and avoiding the occurrence of type-I ELMs [49]. Increased electron heat transport in this ergodic (stochastic) region, due to parallel thermal conductivity in a static tokamak toroidal configuration with destroyed magnetic surfaces [50] was expected to be the main mechanism for enhanced radial transport. To achieve this, magnetic islands could be created in the rational surfaces at the plasma edge by an appropriate set of purposely-built coils so that, by the overlap of these islands in neighbouring flux surfaces, an ergodized edge plasma layer would be created. In this original picture based on transport in an ergodized layer, fine tuning between the perturbation applied to the edge magnetic field and the edge field line pitch so that they would be resonant is advantageous, as it decreases the requirements for the magnitude of the magnetic field perturbation required for edge ergodization and, together with it, the magnitude of the non-resonant components which may have deleterious effects in the plasma. Experiments have demonstrated, however, that in many cases significant effects on ELM behaviour are observed with non-optimum edge magnetic field perturbations and with no or little correlation to edge magnetic field resonance [51, 52]. ELM control and suppression by edge magnetic field perturbation is presently a very active field of research with both on-going experimental and theoretical/modelling activities. Present results indicate that, unlike the initial expectations, the effect of the edge magnetic field perturbations leads to an increase of the edge particle transport with a smaller effect on the energy transport [51]. This control scheme is the only active ELM control scheme so far that has achieved complete elimination of type-I ELMs in conditions of low edge collisionality as required for ITER operation with a small energy confinement degradation [53]. On this basis and the wider experimental results showing significant effects on ELM control in a larger number of tokamaks, a set of in-vessel coils is being considered as one of the two main systems for ELM control in ITER [10]. It is important to understand, however, that there remain issues regarding the application of this ELM control in ITER both concerning its physics basis as well as its compatibility with other scenario requirements which are presently the subject of intense R&D.

Status of experimental investigations

The use of an ergodic field to influence edge transport was originally developed for limiter machines with an Ergodic Divertor (Tore Supra [54]) or a Dynamic Ergodic Divertor (TEXTOR [55]). The onset of increased thermal and particle transport was attributed to overlapping island chains characterized by the Chirikov parameter (island width / island distance) growing beyond unity generating ergodic regions with a chaotic field line pattern [50, 54]. As expected from the edge ergodization and its effect on edge transport, “footprints” for the interaction of the plasma on the limiter develop due to the radial field line excursions, which are in good agreement with predictions from vacuum magnetic field line tracing [55]. Early experimental observations in small divertor tokamaks indicated that edge ergodisation by resonant magnetic perturbations can affect the plasma edge in H-mode and also the ELM behaviour [56, 57, 58]. Edge ergodisation in divertor configurations can be rather efficient with relatively small perturbations due to the strong edge magnetic shear near the magnetic separatrix in X-point configurations which eases the overlapping of islands. As both particle and thermal transport are very low in the pedestal region of H-modes, even a small increase of edge transport in this region might be sufficient to saturate the edge pressure evolution to a lower value so that ballooning-peeling instabilities are avoided and no type-I ELMs are triggered [51, 59], while minimizing at the same time the corresponding loss of plasma confinement [60].

First application of ergodic fields in small divertor tokamaks H-modes regime at high collisionality [56, 57, 58], did not demonstrate the suppression of type-I ELMs, but a transition from ELM-free to type-III ELMy regime, leading to plasma confinement degradation. A major step forward was achieved in DIII-D by demonstrating the avoidance of type-I ELMs in stationary high confinement regimes at high collisionalities applying the perturbation from in vessel "I-coils" with DC operation with main toroidal symmetry n=3 for high triangularity configurations [59] . In these experiments coherent oscillations replace the ELMs producing the same time-averaged transport through the pedestal as is seen during the type-I ELMing phase, but without the large impulsive component typical of the type-I ELMs. These results were first extended to lower collisionalities [61] and then to a range of plasma shapes [62] by adjusting the edge magnetic perturbation and in this case the coherent oscillations in the absence of type-I ELMs were not found. In both regimes, for coil currents above a given threshold, type-I ELMs were eliminated over a wide range of parameters provided that the edge q_{95} was maintained within a given window. An empirical criterion was proposed for the suppression of type-I ELMs at low collisonalities at high triangularities based on the DIII-D experiments and vacuum modelling (i.e. without plasma response) which correlated the disappearance of the type-I ELMs with the width of the edge ergodised region, as characterised by the Chirikov parameter being larger than one in the region of normalised flux $\psi_N \geq 0.835$ [63]. Sound demonstration of type-I ELM suppression in a plasma with ITER-like plasma shape for the Q=10 baseline scenario was demonstrated in this way, as shown in figure 4. Figure 4 shows the ELM fluxes to the outer divertor as measured by the D_α emission for a "natural" (i.e. uncontrolled) type-I ELMy H-mode reference case (upper) and for an experiment in which the ELM control coils are activated between 3.0 and 4.4s. During the phase in which ELM control coils are activated type-I ELMs are eliminated and substituted by an enhanced transport that does not have the coherent features found at high density [62]. A not understood aspect of these results is that the applied magnetic perturbation fields predominantly act on the particle confinement while a much smaller effect is found for the thermal transport. This suggests that either the final magnetic topology that appears in the edge plasma region is significantly different in the H-mode pedestal area from the one observed in Ohmic plasmas, most likely because of the screening of the perturbation applied by the plasma, or that other physics are significantly more important or decrease significantly electron heat conduction along open stochastic field lines [50].

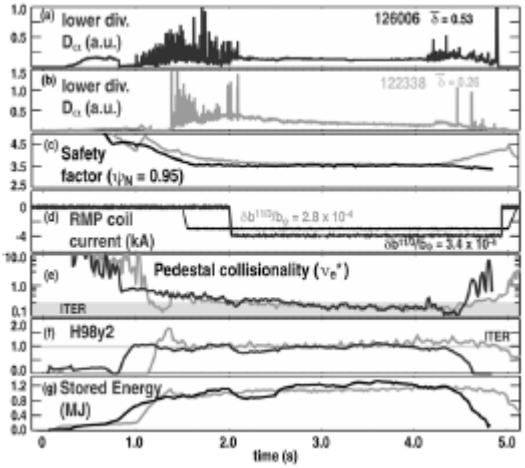

Figure 4. (a) Lower divertor D_α response to the RMP in an ITER-like shape (ISS) plasma with δ = 0.53, (b) lower divertor D_α response to the RMP in a low triangularity plasma with δ = 0.26, (c) q_{95} evolution in the ISS plasmas (black) and the low triangularity plasma (grey), (d) timing and amplitude of the I-coil pulse in each of these plasmas,(e) evolution of the electron pedestal collisionality, (f) H-factor and(g) total stored energy for the low triangularity (grey)

and ISS plasmas (black). The pedestal collisionality and H_{89y2} parameters expected in ITER are indicated in (e) and (f), respectively, forcomparison with the DIII-D data (from [62]).

JET has also demonstrated a reduction of the type-I ELM energy losses, although not full elimination of type-I ELMs by the application of n=1 and n=2 perturbations with external mid-plane coils initially foreseen for error field correction. No complete type-I ELM suppression was observed by application of either n=1 or 2 configurations although the current level in the coils was sufficient to fulfil the empirical criterion derived for DIII-D plasmas. Instead, the frequency of type-I ELMs was observed to increase by more than a factor of 4 resulting in a corresponding decrease of $\Delta W_{ELM}/W$. The largest type-I ELM frequency increases were obtained over narrow operational widows in terms of $q_{95,}$ resembling a resonant-like behaviour as required in DIII-D for complete ELM suppression [64, 65]. Applying resonant n = 3 perturbation allowed to introduce controlled but delayed (about 10 ms with respect to the pulsed coil current) ELM triggering in otherwise ELM-free lithium-enhanced phases at NSTX [66] or transition from low frequency type-I ELMs to smaller more frequent ELMs on MAST at n=3 [67].
A rather common feature of most of the experiments above (with the exception of the high collisionality type-I ELM suppression in DIII-D) is a density reduction ("pump-out"), an increase of Ti and a change in toroidal velocity profile often leading to global plasma toroidal rotation braking. Density pump-out could be minimized at DIII-D and to some level compensated the by injection of small pellets; however pellet fuelling at a high rate lead to the increase of plasma collisionality and the re-appearance of type-I ELMs [62]. Strong gas puffing or pellet fuelling recovered the lost density at JET but at the expense of a reduced confinement (gas) or introducing additional ELMs (pellets) [64].

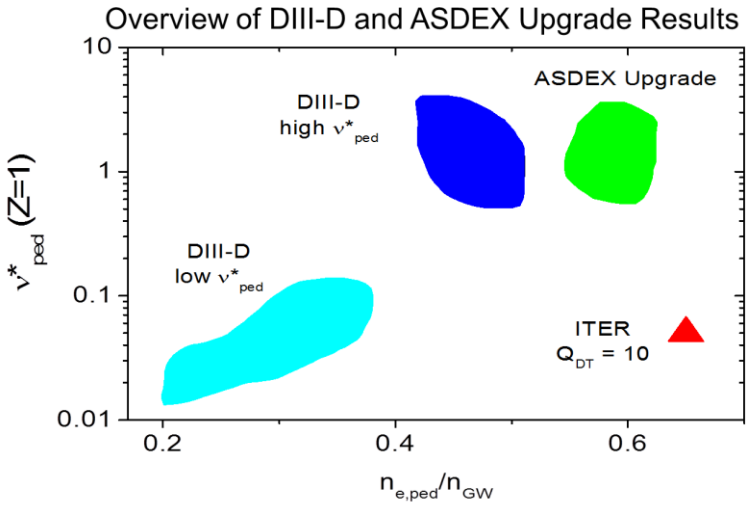

Figure 5. Operational space in terms of pedestal collisionality and pedestal density (normalised to the Greenwald value) for regimes in which type-I ELMs have been eliminated by the application of edge magnetic field perturbations in DIII-D and ASDEX-Upgrade.

ASDEX Upgrade has also achieved suppression of type-I ELMs by applying edge magnetic field perturbations with n=2 symmetry by in-vessel coils. So far, type-I ELMs are eliminated when the plasma density exceeds a given minimum density threshold, which increases with plasma current. Neither density pump-out nor confinement degradation or a significant impact on plasma rotation are observed, while strong ELMs are replaced by high frequency transport events and impurity levels are slightly reduced. Many of these features resemble those of type-I ELM suppression at high collisionalities in DIII-D [53, 59]. However, contrary to DIII-

D, no dependence of the elimination of type-I ELMs on the relative alignment between the edge magnetic field lines and the external edge magnetic field perturbation by the coils have been found. No magnetic islands inside of the separatrix are observed, while at the separatrix strike line splitting is visible, as expected from the existence of an ergodic layer at the edge. Type-I ELM suppression has not been achieved yet at low densities/collisionalities in ASDEX Upgrade. However, the elimination of type-I ELMs has been maintained even when the plasma is fuelled by pellet injection which has allowed increasing the plasma average density in H-mode far above the Greenwald limit [68]. Figure 5 summarises the operational space over which Type I ELMs are suppressed in present experiments.

Status of physics understanding and extrapolation to ITER
Presently, the understanding of the edge magnetic perturbation method for ELMs mitigation/suppression is still at a stage which does not allow a robust physics-based extrapolation for ITER. The basic initial physics basis for the method to act to avoid ELMs in a controlled way (increased thermal transport in the ergodized layer) remains to be demonstrated experimentally, where usually an enhanced particle transport is found. Observations demonstrating the existence of a region with ergodic transport at the edge are now widespread across divertor tokamaks, in which toroidally asymmetric divertor footprints for particle and power fluxes are measured. However, typically, these structures are more predominantly seen in the particle fluxes rather than in the power fluxes and it has not yet been demonstrated that their existence plays a key role on the achievement of ELM suppression itself. In addition, it is not clear whether edge ergodization plays a role on the experiments in which only ELM mitigation is achieved (i.e. increase of the ELM frequency) or whether, in this case, the change in ELM behaviour is associated to changes in edge stability induced by the edge magnetic field perturbation.

A major outstanding issue whose understanding is required to make further progress in this area is to determine what the total 3-d field in the pedestal plasma region is. The total field is given not only by the sum of the external 3-d magnetic field perturbation and the plasma 2-d magnetic field, the so-called vacuum approximation. In addition, 3-d currents can be induced in the plasma rational surfaces that screen/amplify the resonant components of the external 3-d field. The magnitude and location of these response currents are themselves affected by the rotation of the plasma and thus the applied perturbations can be substantially modified from the estimates by the static vacuum model. Recent non-linear MHD modelling shows a significant change of the amplitude of the 3-d perturbation from the one externally applied by currents induced in the rotating plasma [69, 70, 71, 72]. Although, generally, a decrease of the 3-d field is observed (i.e. screening), amplification of certain harmonics is also possible depending on how close to the tearing instability threshold local plasma parameters are [69]. Calculations, which include diamagnetic rotation [70] and neoclassical radial electric field [72] predict that screening of the external field increases for lower resistivity and stronger plasma rotation. Diamagnetic effects and equilibrium electric field are of particular importance for screening in the pedestal region in which large gradients occur. This possibly explains why the vacuum field predictions shows less agreement for H-modes in strongly rotating plasmas (e.g. MAST) and why predicted deposition “footprints” in the divertor are seen on JET and MAST in L-mode, but not in H-mode [73]. Presumably, screening due to the poloidal rotation (ExB and diamagnetic) is larger in the H-mode pedestal region than in L-mode [70]. In DIII-D H-modes, divertor strike zone splitting into helical “homoclinic tangles” is seen [74], but as mentioned above, it is less strong on heat flux compared to particle flux onto the divertor plates. It has been inferred from two-fluid theory that local islands can be formed even in strongly rotating plasmas if ExB poloidal rotation is compensated by electron diamagnetic rotation, leading to a “non-rotating” electron fluid with

respect to the DC perturbation and, hence, vacuum-like islands formation [70, 71]. Investigations on plasma particle transport based on two fluid equations show that, depending on the frequency and direction of plasma rotation, a perturbation of moderate amplitude can either increase or decrease the plasma density gradient around the corresponding rational surface with only sufficiently large perturbations flattening the local density profile [75].

At present, a fully self-consistent MHD theory of the plasma in 3-d external applied magnetic perturbation field including rotation, diamagnetic and neoclassical effects (including poloidal and toroidal viscosity) in toroidal geometry has not yet been developed and this remains a major issue not only to understand the physics processes leading to ELM suppression, as mentioned above, but also to evaluate the effects of 3-d fields at the ITER pedestal.

According to the existing extrapolation attempts to ITER from the modelling of the MHD plasma response, the imposed 3-d magnetic perturbation does penetrate into the outer edge of the ITER plasma but central (parasitic) islands are screened [70, 71, 72]. However, whether the predicted level of penetration and the induced ergodicity are sufficient or not for the achievement of ELM suppression in ITER remains uncertain.

Application of 3-d edge magnetic perturbation to control ELMs in ITER
In view of the large potential for ELM control and the unique demonstrated capability to supress ELMs in a controlled way, a system of ELM control coils is being considered for ITER. The ITER in-vessel ELM control coil system [76] is based on “empirical” guidance from experimental results together with some ITER specific requirements associated with the long pulse/high edge power fluxes expected in burning plasmas reference scenarios. The ITER system consists of 27 coils (3 per vessel sector above, below and at the mid plane, see Figure 6) that can be powered independently to provide edge magnetic field perturbations aligned with the edge magnetic pitch, if this is required for ELM control.

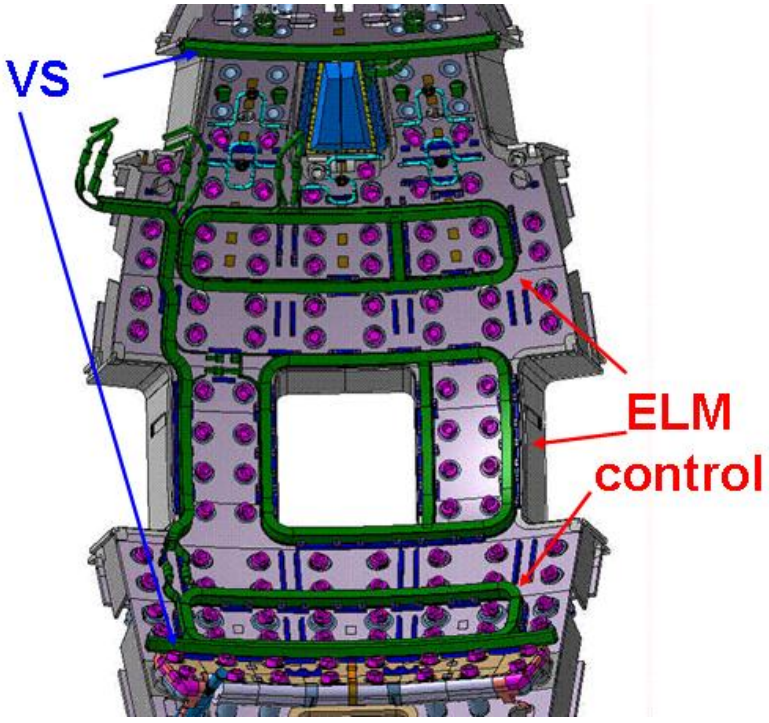

Figure 6: Layout of the in-vessel coils for vertical stability (VS) and ELM control in ITER.

The maximum current capability of the ITER ELM control coil system is 90 kAt and is determined on the basis of the criteria for minimum island overlap that is associated with ELM suppression in DIII-D applied to the 15 MA Q_{DT} = 10 scenario in ITER [63] with an additional 20% margin in the maximum coil current to account for uncertainties. The values of the magnitude of the perturbation field, the magnitude of the various harmonics obtained in the plasma for a current distribution in the coils with n = 4 symmetry and the resulting Chirikov parameter across the plasma cross section are shown in Figure 7 [10].

The level of resonant edge magnetic field perturbation in the pedestal region (~ 35 gauss) is of the order of ~ 6.5 10^{-4} x B_t, while the normal component of the perturbed field in that region is ~ 470 gauss or ~ 9 10^{-3} x B_t. These levels of perturbed field (in the vacuum approximation) are larger than those at which a significant reduction of ELM energy loss is observed even in experiments in which ELM suppression is not achieved. It is also important to note that the distribution of currents in the coils has been optimised to decrease the magnitude of the non-resonant components of the magnetic field, which are only slightly larger than the resonant ones. For other lower current scenarios the requirements of currents in the coils is less stringent and, as an example, a maximum current of only 45 kAt is expected to be needed to meet the empirical criterion derived from DIII-D as estimated on the basis of the Chirikov parameter criterion evaluated with n = 4 harmonics (including the 20% margin in coil current), for ITER operation at 9 MA with Q_{DT} ~ 5 steady-state. A more recent detailed evaluation of the edge field structure in the vacuum approximation has shown that the above estimates provide a conservative estimate of the level of edge ergodisation actually achieved in ITER in the vacuum approximation [77]. This is due to the existence of other harmonics in the field spectrum that contribute to the overlap of islands at the edge and which are not included in the methodology followed in [10]. As a consequence, the estimated margins for the currents in the coils to achieve an equivalent form of the design criterion (based on field line loss fraction including all harmonics rather than the Chirikov parameter for =4 harmonics) can be larger than the 20% originally assumed [77].

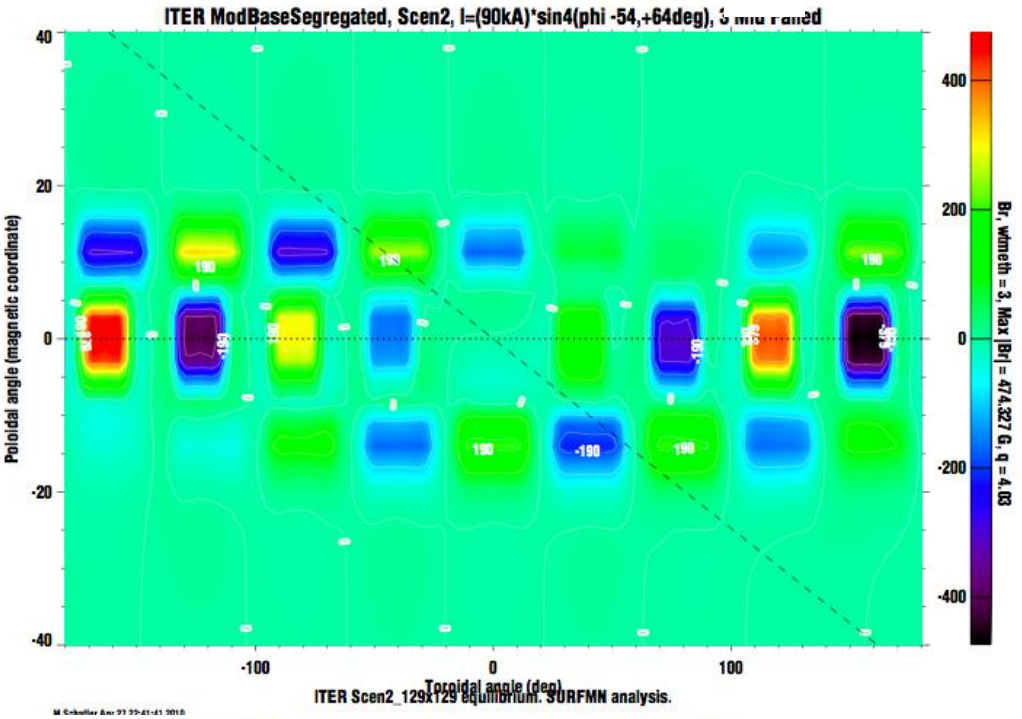
ITER ModBaseSegregated, Scen2, I=(90kA)*sin4(phi -54,+64deg), 3 mid Failed
Poloidal angle (magnetic coordinate)
Toroidal angle (deg)
Br, wlmeth = 3, Max |Br| = 474.327 G, q = 4.03
ITER Scen2_129x129 equilibrium. SURFMN analysis.

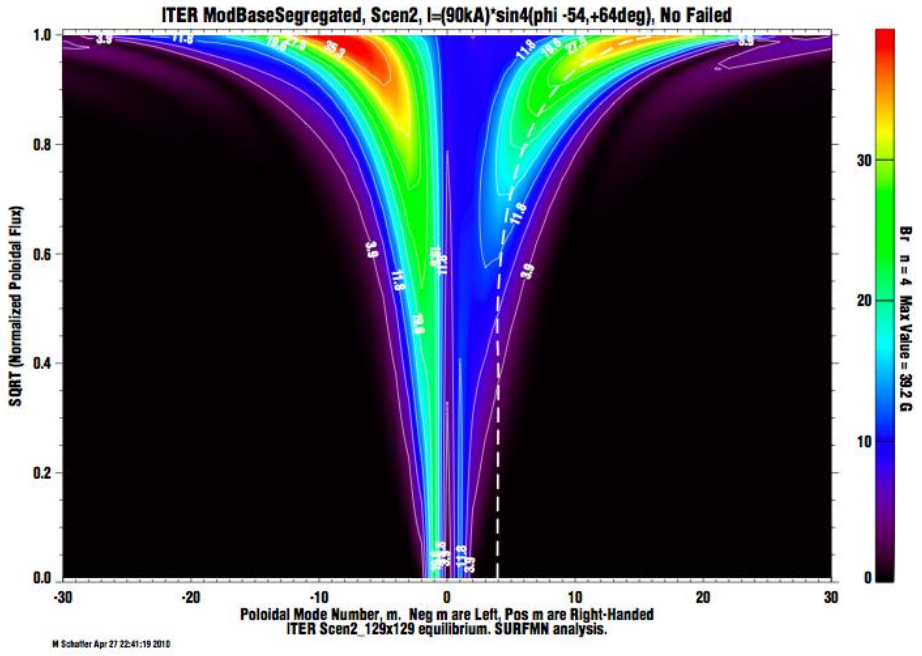
ITER ModBaseSegregated, Scen2, I=(90kA)*sin4(phi -54,+64deg), No Failed
SQRT (Normalized Poloidal Flux)
Poloidal Mode Number, m. Neg m are Left, Pos m are Right-Handed
ITER Scen2_129x129 equilibrium. SURFMN analysis.
Br n = 4 Max Value = 39.2 G
M Schaffer Apr 27 22:41:19 2010

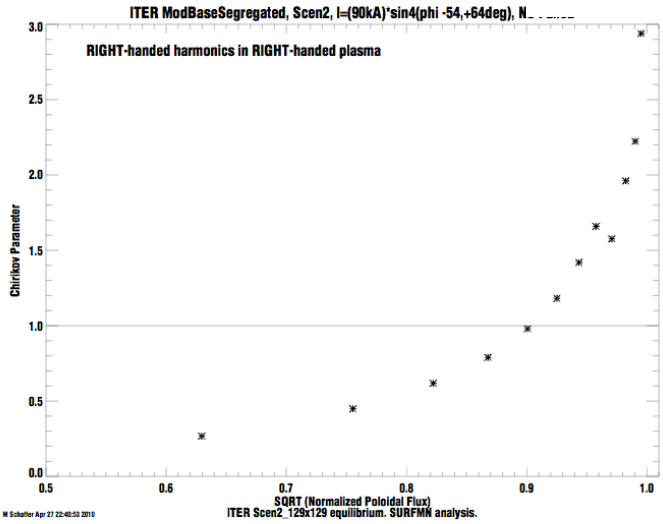

Figure 7: (Top) Total perturbation field normal to the q≈4 surface (one magnetic line is shown dashed for illustration; (Middle) Poloidal harmonic m spectrum of n = 4 helical harmonic amplitudes versus normalised flux. (Bottom) Chirikov parameter versus the square root of the normalised poloidal flux for ITER 15 MA Q_{DT} = 10 scenario and 90 kAt peak current in the ELM control coils.

As identified in experiments and in modelling for ITER [78, 79] and shown in Figure 8, non-toroidally symmetric structures on the particle flux to plasma facing components may exist in ITER (so-called divertor strike point lobes) as a result of the application of edge magnetic field perturbations for ELM control. Such non-toroidally symmetric structures might lead to excessive net erosion rates at the ITER divertor due to the decrease of re-deposition in these areas as they are not toroidally symmetric. The proposed method to mitigate this problem is the rotation of the edge magnetic field perturbation. For the expected power fluxes in ITER and the ITER plasma facing component technology, avoiding excessive thermal cycling of the brazing between cooling channels and the plasma facing elements of the water-cooled divertor PFCs requires that the perturbation is rotated sufficiently fast. Calculations performed for the worst case scenario, in which one of the divertor lobes would have a large spatial extent than the others (which is not unusual as shown for n=4 perturbations in Figure 8), indicated that with a rotation frequency of the heat flux pattern larger than 1 Hz no thermal cycling effects are expected even for the highest power fluxes considered (for power fluxes of 20 MWm^{-2} in the non-toroidally symmetric power deposition areas) [10]. Given the expected use of the coils with n = 4 or n = 3 perturbation symmetry, a frequency of 5 Hz for the power supplies of the ELM coils has been set as a requirement. This allows a full rotation of the heat flux pattern at a frequency of ~ 5/n Hz, which is sufficient to smooth the divertor target erosion while avoiding thermal cycling of the divertor in the worst case scenario described above, even for the cases in which the power flux to one of the strike point lobes (3 or 4 depending on the n) would carry a significant larger power flux than the others at a particular poloidal position.

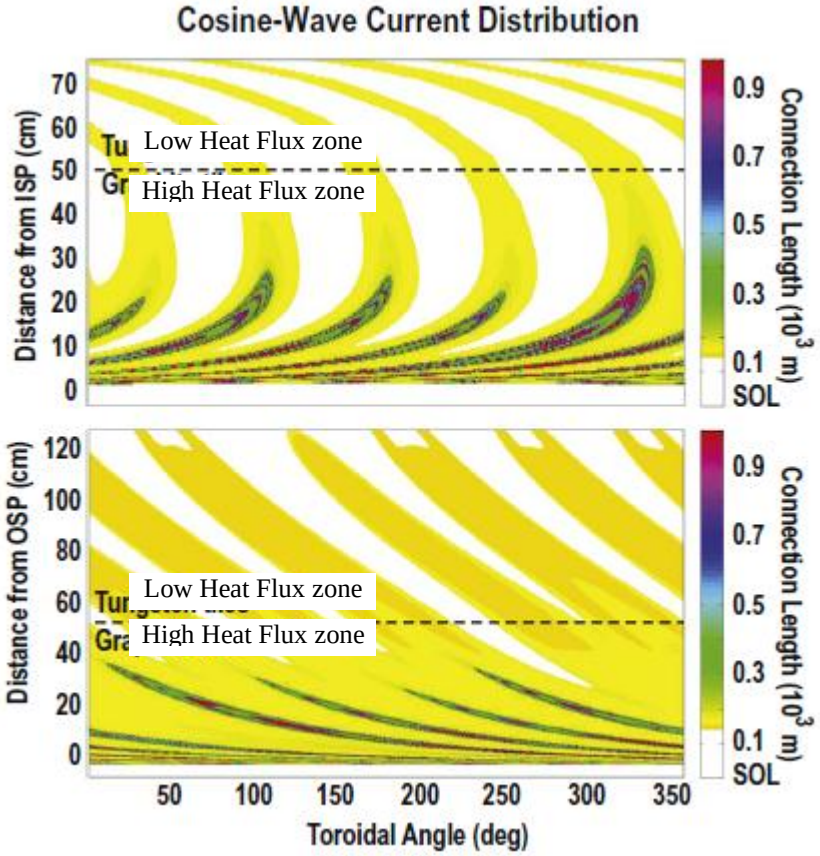

Figure 8: Magnetic ITER divertor footprint pattern with n = 4 RMP spectrum applied to enhance the stochastic layer width. The upper row shows the footprint for at the inner strike line, the lower row shows the footprint at the outer strike line. A cosine-like current distribution with a stochastic layer width of 0.16 is considered in this example [78].

An important issue with regards to the capability for ELM control provided by the in-vessel coils in ITER is the quantification of the performance of the system as a whole in the case of coil malfunction. An initial evaluation has been carried out for ITER by the application of an analytical model for both static and rotating perturbations for the n=4 resonant harmonic. The probability of the ITER system to meet its design criterion has been evaluated in terms of the number of combinations of possible locations of failing coils for which the design criterion would be met to the total number of combinations [10]. It is important to note that, as already mentioned above, other harmonics can effectively contribute to edge ergodization and these are not taken into account in this simple evaluation. As a consequence, the estimates derived with this simple analytic model overestimate the degradation of the performance of the in-vessel coil system under coil failure when compared with calculations that take into account higher order harmonics [77]. In addition, the toroidal phasing between the currents in the various coil rows can be further optimised for the system with failed coils, which increases the level of edge ergodisation lost as coils fail and, thus, further decrease the impact of coil failure on the achievement of the design criterion, but such optimization can be only done with numerical models. Neither of the effects of higher n harmonics nor of mitigation by toroidal phasing optimisation in the case of failed coils has been considered in this simple analytical approximation. Therefore, these analytic estimates should be taken as a pessimistic-conservative estimate for the degradation of the performance of the in-vessel ELM control coil system under failure of some of the coils.

For the purpose of evaluating the expected performance in terms of ELM control, it is assumed that ELM suppression will be achieved in ITER when the Chirikov island overlap parameter, calculated from the vacuum perturbation field with n=4 harmonics, is ≥ 1 on all magnetic surfaces from normalized poloidal flux $\psi_N = 0.835$ outwards [63]. This requirement can be met with a fully functional ELM control coil set in ITER for a maximum current in the coils of 75 kAt and toroidal variations following a cosine law with n=4 and appropriate phase shifts between the upper and lower rows with respect to the mid plane row of coils [80]. To account for uncertainties regarding ELM suppression, a maximum current 20% higher than that required to meet the criteria above is assumed for the design of the coils (i.e. 90 kAt). The result of the analysis is summarised in Figure 9 (from [10]) and shows that the need to rotate the perturbation has clear consequences for the degradation of the performance of the ELM coil control system in ITER as a whole, since in this case at some point of the rotation cycle the current in one or various of the malfunctioning coils is required to be maximum (in absolute value) while no current can be applied to the malfunctioning coils. In the case of a stationary perturbation, the toroidal phase of the currents applied to the coils can be adjusted to minimise the effect of the malfunctioning coils. The toroidal phase can be chosen in this case so that the required current in the malfunctioning coil that could contribute most for the degradation of the perturbation is zero for stationary perturbations. In this way, the failure of an individual coil has no consequence for the performance of the ITER ELM control system if the perturbation is stationary.

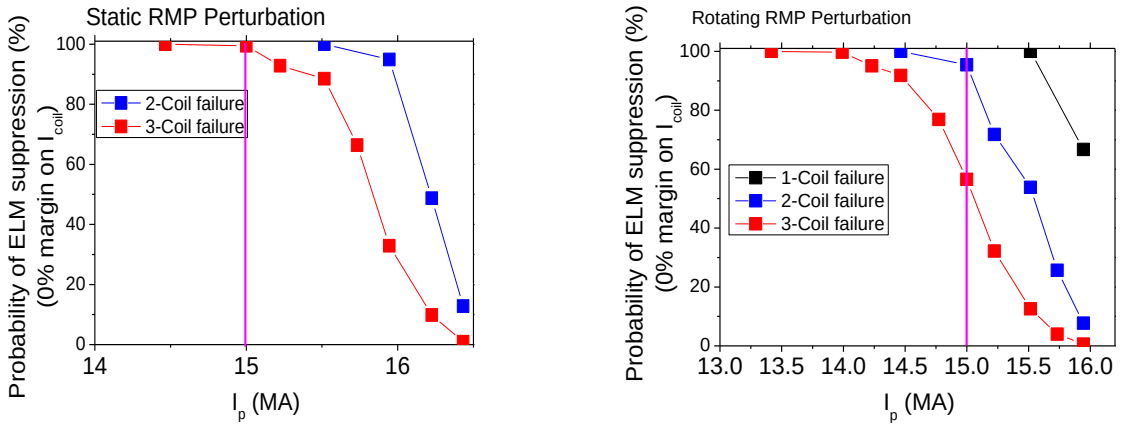

Figure 9: (Left) Cumulative probability for the ITER ELM control coils system operating at maximum current of 90 kAt to meet the ELM suppression criterion (taking as reference the DIII-D ELM suppression criterion) for 2 and 3 malfunctioning coils in ITER versus plasma current for stating perturbations. (Right)) Cumulative probability for the ITER ELM control coils system operating at maximum current of 90 kAt to meet the ELM suppression criterion (taking as reference the DIII-D ELM suppression criterion) for 1, 2 and 3 malfunctioning coils in ITER versus plasma current for rotating perturbations.

On the basis of this pessimistic-conservative analytical study, it can be concluded that the capability for ELM suppression of the ITER ELM control coil system (on the basis of the DIII-D ELM suppression criterion) is maintained for plasma currents above 14.5 MA for the vast majority of cases in which up to 3 coils malfunction, even if it were necessary to rotate the edge magnetic field perturbation. It is also important to note that even for the worst possible case considered in this analysis (three midplane malfunctioning coils for which maximum current is required to be maximum), the resonant edge magnetic field perturbation in the pedestal region is expected to be ~ 23 gauss, which is of a magnitude ($4.3\ 10^{-4}$ x B_t) for which a significant reduction of ELM energy loss is observed in present experiments.

An outstanding issue concerns the application of this scheme for ELM control in the non-active ITER operational phase, particularly for Helium (He) H-mode plasmas. The foreseen level of plasma current at which this regime is expected to be explored in ITER is ~ 7.5 MA; much lower than that for which the ELM control coil system is designed (15 MA) indicating that there is a large margin for the demonstration of ELM control in these conditions in ITER. However, experiments in He H-mode plasmas in JET [81] and DIII-D [82] have shown that the level of edge magnetic perturbation required to achieve ELM control in He plasmas is higher than that for D plasmas. Therefore, the margin available to demonstrate ELM control in He plasmas in ITER may be smaller than originally anticipated. More experiments in this area are needed to quantify this difference in ELM control requirements between D and He H-mode plasmas.

In addition to R&D towards the understanding of the physics basis for ELM control and suppression by edge magnetic field perturbation (including plasma response effects and effects of the non-resonant components on plasma rotation), other issues must be studied to ensure the compatibility of this ELM control scheme with ITER scenarios and requirements. This is the subject of experimental R&D in present devices and modelling; whose significant progress is reported below:

a) The influence of the application of edge magnetic field perturbations on H-mode access has been studied. It has been found that application of edge magnetic field perturbations before the L-H transition can increase the power required for access to H-mode by up to 40%, with the strongest effects seen when the perturbation is well aligned with the edge magnetic field [83]. On the other hand, experiments in DIII-D have recently demonstrated the access to a suppressed ELM regime from L-mode through a type-III ELMy H-mode while avoiding large type-I ELMs, which would be highly desirable in ITER [84]. The above evidence indicates that flexibility in the system should be maintained to be able to access the H-mode with no edge magnetic field perturbation and switch it on after the L-H transition or to switch the perturbation on while in L-mode but only optimise the alignment between perturbation and field once the H-mode transition has occurred in ITER. In this way, a better control of the evolution from L-mode to a high confinement H-mode while avoiding type-I ELMs may be achievable.

b) The application of edge magnetic field perturbations typically leads to a decrease of the plasma density and a decrease of the plasma confinement by ~ 10%, with the notable exception of the high density elimination of type-I ELMs in ASDEX-Upgrade [52] and DIII-D [53,59] in which no decrease of plasma density was observed and very small energy confinement deterioration was found. Recovery of the plasma density by gas puffing or pellet fuelling is possible but without recovery of the lost plasma energy. In the case of ELM suppression at low collisionalities in DIII-D, recovery of the plasma density by gas puffing leads to the re-appearance of small high frequency ELMs [85]. Experiments in DIII-D have also shown that the application of edge magnetic field perturbations with varying strength in time after the L-H transition may be an avenue for further R&D to decrease or avoid the decrease of the plasma density associated with the application of RMPs [84]. Pellet fuelling can also be used to recover the lost density but this leads to the triggering of ELMs (in ELM controlled regimes) [64] or edge transients or ELMs (in ELM suppressed regimes) [62], but the systematic characterisation of these plasma operational regimes remains outstanding. New experiments in high density regimes without type-I ELMs in ASDEX Upgrade show that the plasma density can be increased by pellet injection without triggering of type-I ELMs [68], which indicates that the application of edge magnetic field perturbations may have a stabilizing effect to the perturbations induced by the pellets at the plasma edge. Understanding of the physics

mechanisms leading to the observed behaviour and of their relevance in ITER high density/low collisionality regimes remain subjects of R&D.

c) Compatibility of ELM control/suppression by edge magnetic field perturbation and stationary power flux and erosion control. Besides the effects on the pedestal/SOL described above, application of edge magnetic field perturbations is expected to affect edge particle and energy transport and lead to the appearance of non-toroidally symmetric structures at the divertor target. Evidence for this has been documented in DIII-D [74, 79], NSTX [86], and MAST and JET (in L-mode) and models have been developed that are able to reproduce some of the experimental features [87]. Although the extrapolation of the existing experimental and modelling results to ITER is not straightforward and more R&D is required [78], they provide evidence that significant particle and power fluxes may reach the ITER divertor in non-toroidally symmetric structures and at relatively large distances from the separatrix and this should be taken into account into the ITER design. The major issue that needs to be studied in detail for ITER is to which level ELM control by RMPs affects the divertor conditions for high density/high radiation conditions. Initial results from high density operation in DIII-D [59], NSTX [88], ASDEX-Upgrade [52] and JET [65] and high divertor radiation in DIII-D [89], indicate that a high density/highly radiating divertor can be obtained with controlled ELMs although elimination of type-I ELMs has only been demonstrated in ASDEX-Upgrade and DIII-D under these conditions so far.
d) Sustainment of ELM control/suppression by edge magnetic field perturbation in conditions with varying q_{95}. This is intrinsically related to the need to maintain a resonant perturbation to achieve ELM suppression. For operational reasons, in ITER it is foreseen that in most high Q scenarios the H-mode will be accessed in the current ramp-up before the plasma current flat top and it will maintained in the ramp-down. The typical value of the current at which H-mode will be accessed to/exited from is 2/3 of the plasma current flat top, which implies that ELM suppression should be maintained while the edge q_{95} changes from/to 1.5 to 1.0 of its flat top value during the ramp-up/down. While timescales in ITER are long, which eases the control issues, and the system of ELM control coils is being designed with enough flexibility to have the capability to maintain good alignment of the perturbation with the changing magnetic field pitch angle in these transient phases, an experimental demonstration that such degree of ELM control is possible in ramped current phases is still outstanding.

5. Pellet injection

Injection of cryogenic solid pellets is a method of the ELM pacing category which achieves ELM control by increasing the ELM frequency, and relying on the inverse dependence of the ELM energy loss on frequency, so that the frequency is increased until the required level of ΔW_{ELM} is achieved. Originally, pellet injection was intended for efficient fuelling of plasmas in tokamaks but it turned out that fuelling was much less efficient than originally foreseen in H-mode plasmas. This is due to the triggering of ELMs by the pellets as they enter the plasm,a which has been observed in a large number of tokamaks. In cases where the pellet timing and frequency was such that they induced additional ELMs and shortened the period between ELMs, it was found that indeed the pellet triggered ELMs expelled less energy from the plasma that the corresponding uncontrolled ELMs. This result motivated the development of the so-called ELM pacing by pellet injection as ELM control technique. In this control scheme ELMs are triggered at a control frequency which is determined by the injection of the pellets. Because the initial pellet launchers were designed for fuelling purposes (i.e. large pellets that penetrate as deep as possible in the plasma) most of the experiments so far have

been carried out with these systems, which have the drawback of a substantial fuelling of the plasma being caused together with the control of ELMs. Newer systems optimized for pellet pacing with smaller pellets have now become available and are being used to determine the potentialities of this control scheme at the level required for ITER.

Pacing scenario investigations

A first proof-of-principle demonstration of ELM pacing and ELM control was carried out at ASDEX Upgrade [90]. By injecting pellets with a frequency a factor of 2-3 times higher than the natural, or uncontrolled, ELM frequency full control of the ELMs was achieved with the pellet rate f_{PEL} determining the ELM frequency f_{ELM}. A full control sequence from the initial f^0_{ELM} into an about 2 s long phase with $f_{ELM} = f_{PEL} \approx 2\times f^0_{ELM}$ and back to f^0_{ELM} was demonstrated. Experiments also showed that, in these conditions, the ELM frequency follows instantaneously the pellet injection frequency (f_{Pel}) as soon as the train of pellets starts reaching the plasma. The ELM energy loss is found to decrease while conserving the relation $\Delta W_{ELM}/W \times f_{ELM} \times \tau_E = \text{const.}$ [18], but this only occurs once steady state conditions are established. In ASDEX Upgrade this corresponds to a transient period of ~ 0.2 s (2-3 τ_E) in which the ELMs adapt to the new frequency driven by the pellets, following which new stationary plasma conditions are established with typically a 10% lower plasma energy. An example of this dynamic behavior can be seen in figure 10. The observed confinement loss can be attributed to the convective losses introduced by the pellets which, in these experiments, were rather large and optimized for fuelling. During the stationary phase the controlled ELMs show no major difference compared to natural or uncontrolled ELMs of the same frequencies but, hence, different plasma edge parameters. The empirical correlation usually observed for uncontrolled ELMs between plasma edge parameters (density, temperature, collisionality, ...) and ELM frequency is, thus, broken for ELMs controlled by pellet pacing. In this case, the ELM frequency becomes a free parameter that can be controlled by the injection of more or less frequent pellets [91].

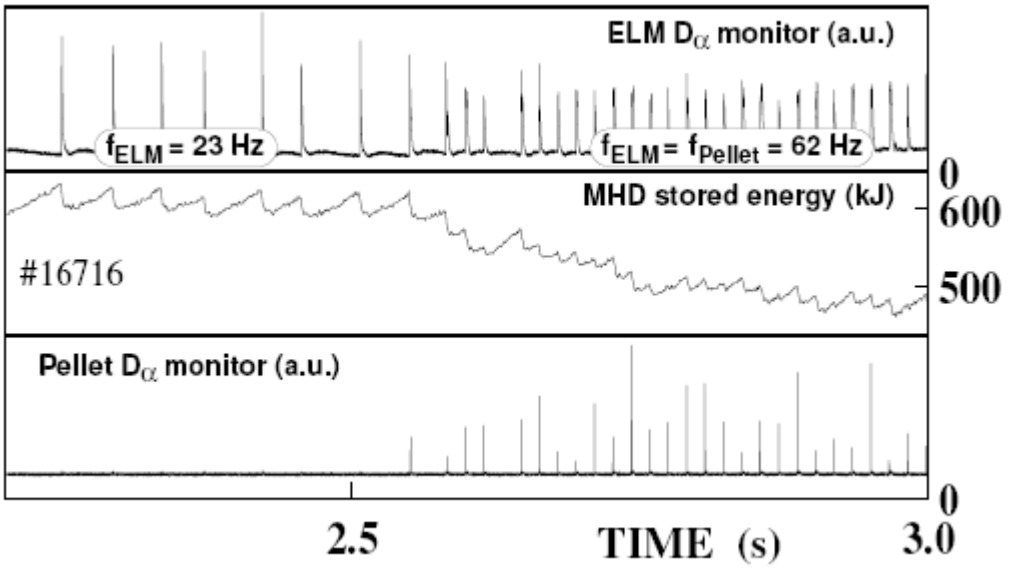

Figure 10: Onset of pellet pacing sequence in ASDEX Upgrade: the ELM frequency follows immediately the pellet rate resulting in a ~ threefold increase of the frequency and a corresponding ELM energy loss reduction. Additional convective losses associated with the expulsion of pellet injected particles (fueling size pellets are used in this experiment) cause a mild confinement loss [90].

Full synchronization of ELMs with injected pellets ($f_{ELM} = f_{PEL}$) was also achieved in JET, confirming that pellet pacing works in the largest existing tokamak [92]. An ELM frequency increase up to a factor 4 accompanied by a corresponding ELM energy loss reduction was achieved for the "ITER-like" baseline scenario. However, here the increase of f_{ELM} was partially due to secondary effects of pellet fuelling. It was also demonstrated at JET that by an early start of the injection of pacing pellets, the first large spontaneous ELM after the L-H transition can be avoided [93]. DIII-D initially demonstrated an enhancement of the initial uncontrolled ELM frequency by pellet injection factor of about 5, also accompanied by a strong reduction of the ELM size [94]. However, in these experiments it was found that the frequency of the controlled ELMs was larger than that of the pellets indicating that part of the ELM frequency enhancement must be due to secondary effects, although the injection of pellets does not show a noticeable impact on the density. More recent experiments from DIII-D, with an optimized pellet injection system for ELM control, [95] have achieved a frequency enhancement of the natural ELM frequency by a factor of 10-15 in which all ELMs are triggered by pellets and with no significant fuelling into the plasma. Also recently, pellet ELM control in an early heating phase, while the plasma undergoes the L-H transition during a current ramp up with still changing shape and q_{95} was demonstrated in ASDEX Upgrade. Pellets reaching the plasma immediately after the H-mode transition do trigger ELMs despite an edge pedestal just starting to evolve and being still far from its final (i.e. edge MHD unstable) parameters. In these experiments there was neither an impact on the transition power threshold nor on the confinement achieved in stationary conditions [96].

Status of physics understanding and extrapolation to ITER

A key issue regarding the application of this technique in ITER is the determination of the physics mechanisms and the associated requirements for the pellets to ensure that ELMs will be triggered in ITER, as well as their compatibility with other scenario requirements. To this end, dedicated experiments were carried out in several tokamaks to understand the underlying physics of the process that leads to ELM triggering by the injection of pellets and their applicability for ELM control across various plasma regimes. These investigations cover a wide range of plasma regimes, as well as of plasma and pellet parameters. There is a high level of consistency in the results of these experiments carried out in different machines, which provide a sound experimental basis for ELM triggering, although it is clear that most of the experiments were conducted in conditions far from ITER relevant requirements. As an example, the results from these experiments concerning the required pellet penetration for ELM triggering are summarized in figure 11.

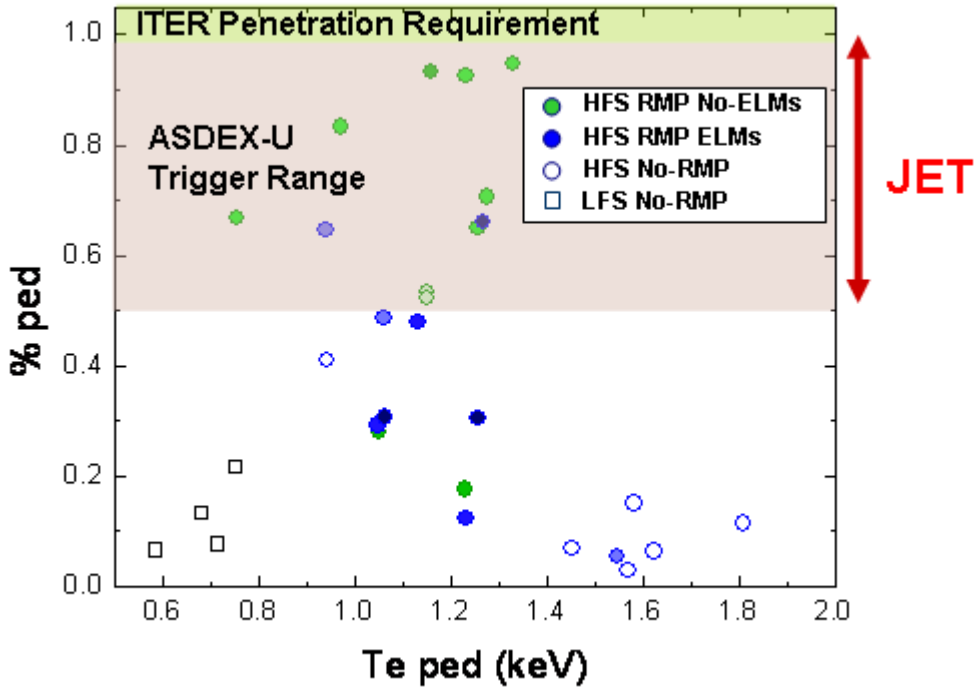

Figure 11: Measured pellet penetration normalised to the distance from separatrix to pedestal top at which ELMs are triggered for a series of plasma and launching geometries (HFS and LFS) in DIII-D versus pedestal temperatures [94]. For comparison the pellet penetration at which ELM triggering is observed in JET and ASDEX Upgrade are shown [90, 93].

Characteristics of triggered and paced ELMs have been intensely analyzed, usually characterizing them with respect to uncontrolled ELMs, and it has been found that pellet triggered ELMs are very similar to uncontrolled ELMs of similar characteristics with only minor changes of e.g. MHD characteristics compared to their uncontrolled counterparts [97]. In plasma regimes without ELM activity, e.g. in the QH mode or for plasmas operated below the H-mode threshold, no ELMs are triggered by the injection of pellets. In cases where ELM control is achieved by another control approach (e.g. radiative edge cooling [46], edge magnetic field perturbation applied only to reduce ELM size) the additional ELMs triggered by the pellets are also very similar to the spontaneous events occurring during these phases; in particular the already reduced ELM size is maintained. Thus, it seems that pellet pacing is compatible with other schemes for ELM control. In the case of ELM suppression this is less obvious as the behavior may be different for low and high collisionality conditions as explained in the previous section. In such conditions it is not yet fully demonstrated that the injection of pellets may not lead to the triggering of ELMs, which would not be acceptable in ITER for suppressed ELM regimes at low collisionalities.

In order to further the understanding of ELM triggering by pellets, the non-linear MHD code JOREK was applied to study the triggering of ELMs by pellets [98]. The results obtained with a simplified model for the ablated pellet indicate that a large enough pellet injected into an H-mode pedestal can destabilize a ballooning-type mode triggering an ELM-like event. Modeling results provide a good qualitative description of the ELM trigger process. Initially, the pellet leads to a large density perturbation expanding along the field line, then fast electron heat conduction increases the pressure inside this partially ionized plasmoid. For a large enough pellet source, this plasmoid deforms into a single filamentary structure moving density outwards while the ballooning instability spreads poloidally over the whole flux

surface. No quantitative prediction of the required magnitude of the pellet driven perturbation to trigger an ELM is possible with such simplified model. However, modeling indicates that the critical amplitude for the pellet perturbation necessary for the onset of the ELM instability is very similar for high field side and low field side pellets [99]. The evolution of the pellet ablation plasmoid into a first ELM filament has been indeed observed by fast framing camera measurements at JET [100] and DIII-D [94]. In addition, modeling predicts that this initial single filament can lead to a localized power deposition at the divertor, which has been confirmed by experimental measurements at JET [101]. Further investigations regarding this localized power flux are needed with the injection of small pellets, since the sizeable effects described above have been observed so far for large pellets optimized for plasma fuelling and not for ELM triggering.

From the scientific point of view, the major issues which need to be resolved with a view to the application of this technique to ITER and for its integration with other scenario requirements are:
a) the quantification, at ITER relevant levels of frequency enhancement of the uncontrolled ELM frequency (> 10), of the confinement reduction by pellet pacing resulting from its effect on the average pedestal pressure and from the increased particle and energy outflux associated with the expulsion of particles in the pacing pellet.
b) the determination of the minimum pellet size and optimum injection velocity and injection location for the triggering of ELMs with a view to minimise the additional fuel throughput that is required for the use of this ELM control technique.
c) the additional energy fluxes to the divertor and main wall associated with the expulsion of the particles in the pacing pellet by the ELM which it triggers. Here the major concern is related to observations of concentrated heat loads by filaments expelled in an initial phase of the ELM triggering process, which could carry a substantial fraction of the pellet particles and which could cause sizeable toroidally and poloidally localised heat loads.

In addition there are two important issues which are related to the approach of ELM pacing as an ELM control technique in ITER and obviously important, but not specific to the use of pellets to pace the ELMs :
d) the evaluation of the reduction of the peak ELM energy load and timescales for ELM energy deposition at the divertor for triggered ELMs at ITER relevant levels of frequency enhancement (> 10). Here the major concern is connected with the observed dependence of the effective ELM energy deposition area on ELM size [102] which, if very strong (i.e. $A_{ELM} \sim 1/\Delta W_{ELM}$), would render all ELM pacing techniques not viable for the reduction of the peak ELM energy flux at the divertor.
e) to determine whether or not the decrease of $\Delta W_{ELM} \sim 1/f_{drive}$, where f_{drive} is the frequency of the external ELM trigger (f_{PEL} in this case of pellets) applies for any value of the driving perturbation leading to ELM triggering. Here the concern is that for most observations in which ΔW_{ELM} is decreased by controlled triggering of ELMs, this decrease comes mostly from the decrease of the perturbation that the ELMs cause to the plasma temperature with a much smaller decrease of the perturbation caused to the plasma density. If this holds to high frequency enhancements, it would set a minimum limit to the reduction of ΔW_{ELM} that can be achieved by the pacing techniques. This would be that of the purely convective ELMs in which only the plasma density is modified by ELMs with the energy loss being purely due to the associated convection of energy with the ELM particle loss [103]. Increasing the ELM frequency beyond the one required to achieve convective ELMs would not reduce further the ELM energy loss but rather increase the power outflux from the ELMs thus severely deteriorating plasma confinement.

The assessment of these effects and the optimisation of the pellet injection location and size to achieve the required level of ELM control and the required plasma fuelling is the subject of on-going experimental R&D with new pellet injectors specially designed for ELM pacing. These new injectors are being used to investigate the requirements and consequences of pellet pacing of ELMs for ITER-like conditions in JET, AUG and DIII-D. Only very recently, these novel systems designed and built for delivery of smaller pacing size pellets have become available. However, these systems are technologically challenging, since the production and transfer of such small pellets (for existing tokamaks pacing pellets should have sizes in the mm or even sub-mm range) is a difficult task and the required technology is only now reaching a matured state.

Application of pellet pacing for ELM control in ITER

ELM triggering and frequency control by pellet pacing is a robust and reproducible effect, observed in all major tokamaks. Although a firm demonstration of the required ELM frequency enhancement and, even more critical, of a sufficient reduction of the divertor power fluxes has not yet been obtained, it is likely that pellet pacing of ELMs for ELM control will work in ITER at least within some operational range. Thus, pellet pacing of ELMs is being considered as one of the ELM control schemes to be applied in ITER. The pellet injection characteristics required for triggering of ELMs are incorporated into the pellet injection system of ITER which is also designed to allow efficient fuelling if the plasma [10].

In view of the experimental results above, penetration of the pellet to the pedestal top in ITER reference Q=10 scenarios is being considered as a conservatively safe guidance for the requirements for ELM triggering by pellets in ITER. This, together with other assumptions derived from the experimental observations, such as the size of the density perturbation required to trigger an ELM, has been used to estimate the requirements regarding pellet triggering in ITER by injection of pellets from the LFS [104], as shown in figure 12. For the design velocities of the ITER pellet injector (300-500m/s), the required pellet content for ELM triggering provided by this empirical guidance is estimated to be in the range 1-4x10^{21} particles/pellet (~16-66 mm^3) which is within the range foreseen for the ITER injector (17-92 mm^3) [10]. As already mentioned, the physics basis for such choices remains to be developed and initial steps in this direction are being undertaken by the application of non-linear MHD codes to the simulation of ELM triggering with appropriate modelling of the ablating pellets [105].

Because of their shallow penetration in ITER, the fuel injected by ELM pacing pellets is expected to be expelled by the triggered ELMs and not to contribute significantly to the core plasma fuelling. Despite this, the particles injected in these pellets can contribute considerably to the total plasma particle throughput; e.g. pellets with 2 x10^{21} particles/pellet injected at 30 Hz provide an outflow of ~ 6 x 10^{22} s^{-1} or 120 Pam^3s^{-1}. This flux is in addition to the particle outflow caused by controlled ELMs and, thus, a significant additional particle throughput that needs to be handled by the pumping and detritiation systems. As described above, controlled ELMs in ITER are expected to be fully convective, i.e. cause no modulation of the edge plasma temperature (i.e. $\Delta T_{ELM} \sim 0$) and have frequencies in the range $f_{ELM} \approx 30-60$ Hz for Q~10 operation. The particle loss in these ELMs is expected to be ~ 4x10^{20} particles/ELM, leading to an average particle outflow of $<\Gamma_{ELM}>= f_{ELM}\Delta N_{ELM} = 1.2-2.4\times10^{22}$ s^{-1} or 24 – 48 Pam^3s^{-1}. This increased particle throughput during the ITER inductive Q_{DT} ~10 pulses associated with ELM control is included in the requirements for the ITER vacuum and tritium systems, which are designed to cope with a maximum average throughput for the inductive scenario of 200 Pam^3s^{-1} with peak values of 400 Pam^3s^{-1}, but it is obvious that the approach to ELM control by pellet pacing in ITER places a significant burden to the fuel cycle and further

R&D should be carried out to determine how this can be minimised (i.e. optimising pellet size to the minimum, etc.) [10].

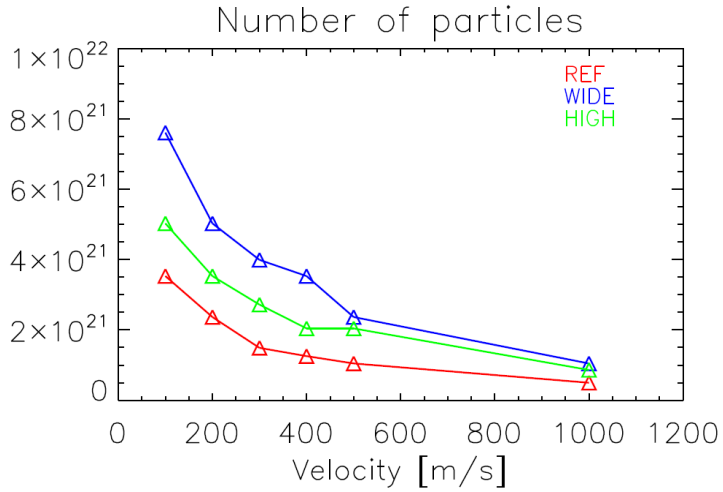

Figure 12: Size of the pellet (number of deuterons) required to reach the ITER pedestal top and trigger an ELM as a function of the velocity for the LFS injection line for various assumptions regarding the pedestal plasma and pedestal widths [104].

Detailed estimates of the pellet pacing requirements for I_p < 15 MA operation in ITER have not yet been carried out but they are expected to be less demanding than those for Q=10 at 15 MA [10]. This is due to the fact that:
a) The area for energy deposition due to ELMs is expected to be larger at lower currents (assuming that the broadening of the ELM energy deposition area is related to the between-ELM SOL power width, which is expected to scale as ~ I_p^{-1}), thus allowing a larger ΔW_{ELM} for controlled ELMs for a given maximum ELM energy deposition density, which is set by material damage limits.
b) The uncontrolled ELM energy loss is expected to be smaller for the lower current plasmas, mainly because the pedestal energy is expected to scale as W_{ped} ~I_p^2 but also because the pedestal collisionality is expected to increase as ν^*_{ped} ~ I_p^{-1} and this reduces the uncontrolled ELM size for a given W_{ped}.
c) Because of a) and b) the required ELM frequency enhancement for controlled ELMs with respect to uncontrolled ELMs decreases for lower currents in ITER as summarised in Table 1.
d) In addition, the uncontrolled ELM frequency in ITER is only expected to increase mildly with decreasing plasma current because the alpha heating decreases with decreasing current and with it the edge power flow which, in turn, leads to a decrease of ELM frequency for a given uncontrolled ELM loss.
e) The pedestal plasma densities and temperatures are expected to scale approximately linearly with I_p and thus will be lower at lower currents, which is expected to facilitate pellet penetration and decrease the size of the pellet required to trigger an ELM as found in JET experiments [10].

Scenario	**P_{SOL} (MW)**	**B_t (T)**	**$\Delta W_{ELM}^{uncontrolled}$ (MJ)**	**$f_{ELM}^{uncontrolled}$ (Hz)**	**$\Delta W_{ELM}^{controlled}$ (MJ)**	**$f_{ELM}^{controlled} = f_{pellet}$ (Hz)**	**$f_{pellet}/f_{ELM}^{uncontrolled}$**
Inductive scenario 15 MA	100	5.3	20	1.0-2.0	0.7	30-60	30
Hybrid scenario 12.5 MA	100	5.3	12.5	1.5-3.0	1.0	20-40	13
Steady-state 8-9 MA	80	5.3	3.9	4-8	2.1	8-16	2
10 MA H-mode	50	5.3	7.0	1.5-3.0	1.4	7-14	4.6
7.5 MA H-mode	50	2.65	4.0	2.5-5.0	1.7	6-12	2.4

Table 1: Expected uncontrolled ELM energy loss and frequency and required controlled ELM energy loss and associated frequency (assumed to be equal to the pellet injection frequency for pellet pacing) to avoid divertor target damage by ELMs in the absence of broadening of the power flux during controlled ELMs. The last column summarises the required pellet frequency as a ratio to that expected for uncontrolled ELMs [10].

Besides the outstanding issues related to the physics basis of this technique and its compatibility with other ITER scenario requirements and fuel throughput limitations described above, two other important issues remain to be addressed for the practical application of this technique to ITER and for its use during the initial non-active phase of operation:

a) A technically outstanding issue is the need for a reliable injection of several tens of thousands of pellets per ITER discharge, as required for 15 MA $Q_{DT} = 10$, with sufficiently uniform parameters to ensure the triggering of an ELM for every pellet injected. This constitutes a significant extrapolation from today's experience and requires further R&D on pellet injection technology.

b) Another outstanding issue, from the point of view of the application of this technique to ELM control from the initial operation, concerns the application of this technique to He plasmas with H pellets. As described in Table 1, control of ELMs in H-mode plasmas at 7.5 MA, which are expected to be achieved in ITER with helium plasmas, may require the reduction of ΔW_{ELM} down to 1.7 MJ, which corresponds to a pellet pacing frequency of f_{pellet} = 6 - 12 Hz. Even for a moderate size pellet of 17 mm^3, the associated hydrogen throughput can reach ~ $10^{22} s^{-1}$ and this may cause significant dilution of the He plasma, as shown by B2-Eirene modelling [107], which in turn may affect adversely the H-mode behaviour (H-mode power threshold is higher for H than for He plasmas) [108]. Depending on the exact pellet size and pellet pacing frequency required and the deleterious effects of H on He plasma H-mode plasmas in ITER, demonstration of pellet pacing by H pellets in ITER He plasmas may be restricted to short time intervals only. This may prevent the study of some of the scenario integration issues of pellet pacing described above during this initial phase of non-active operation, which should be then addressed when DD operations take place.

6. Fast plasma movements

The method of applying a fast (mostly vertical) plasma movement to control the ELM behaviour has been utilized in many tokamaks and is called by several denominations: magnetic triggering, wobbling, kicking or joggling. This ELM control scheme aims to trigger ELMs at an externally imposed frequency with the consequent decrease of the ELM energy loss and it is, thus, an ELM pacing approach to ELM control. The physics basis behind this scheme is that a rapid motion of the plasma column can change the edge plasma parameters so that they can bring them in a region where they are MHD unstable causing an ELM to occur. By causing this instability to occur at a prescribed ELM frequency, the ELM energy loss is reduced in inverse proportion to the increase of the prescribed frequency of the vertical motion. The first successful demonstration of this technique was achieved at the TCV tokamak and the physics interpretation of the results indicated that the triggering of the ELM instability was the change of the edge current by the induction of currents as the plasma was moved vertically in an up-down asymmetric magnetic flux pattern [109]. This scheme for ELM control was reproduced in several other devices. In some devices, notably JET, the technique has reached a stage of maturity that allows its routine use for ELM control purposes. The initial physics basis derived from the TCV experiments has not been confirmed in the other tokamaks in which the technique has been demonstrated and other explanations for the triggering of ELMs by displacement are under investigation, such as the effect of the modification of the plasma shape when the plasma is moved in altering the edge stability boundary and leading to the triggering of ELMs. Since this ELM control method relies on the use of the vertical plasma position and stability control systems which are available in all tokamaks, its implementation is relatively straightforward either by using these systems as they are or with small modifications to the hardware or control software. The application of this technique, however, incorporates some risks, e.g. by causing additional thermo-mechanical stresses in the coils used to move the plasma vertically as well as an increased risk to vertical displacement events due to the loss of vertical stability control, which is usually maintained by the same coil system that applies the plasma movement. These and other considerations will be analysed in more detail below when the application of this scheme for the control of ELMs in high Q scenarios in ITER is discussed.

Status of experimental and modeling investigations

As already mentioned this scheme for ELM control was first developed (and named ELM control by magnetic triggering) and demonstrated at the TCV tokamak [109]. Coils which were routinely used for vertical plasma position feedback stabilisation were driven by a short voltage pulse causing a small vertical excursion of the plasma column. The plasmas to which this technique was applied were ohmically heated H-mode plasmas with stable type-III ELMing phases with an ELM frequency of ~ 250 Hz in upper or lower single null magnetic configurations. The naturally up-down asymmetric flux pattern of the single null is, hence, pushed against or away from the current in the poloidal field coils responsible for creating the X-point as the plasma is moved vertically. It was found that ELMs were triggered when the plasma was moving away from the X-point, while stabilization was observed during the phase of plasma motion towards the X-point, irrespective operation in upper or lower null configuration. As mentioned above, this is in good agreement with the expectations from the application of Lenz's law implying that a negative surface voltage and, hence, negative edge current will be induced when the plasma moves towards the X-point which is expected to increase edge stability and avoid ELM triggering and the opposite trend when the plasma moves in the opposite direction. It was found that the ELM frequency could be made to match that of the plasma movement (i.e. frequency locking) in the range of 140-330 Hz provided that the cyclic plasma excursion was sufficiently large. Larger peak-to-peak amplitudes of the perturbation resulted in a wider frequency band around the unperturbed ELM frequency

where locking was achieved, as well to reduce the scatter of the ELM frequency with respect to that of the plasma movement frequency.
The technique was also demonstrated to be suitable for the triggering of type-I ELMs with its first demonstration in ASDEX-Upgrade. In these first experiments, the movement of the plasma was obtained by a suitable request to the feedback controlled plasma position and shape control system, which was found to be capable to perform a smooth, almost sinusoidal, vertical wobbling of the plasma at a frequency in the range 30 to 90 Hz [110]. Type-I ELM frequency control by locking to the wobbling frequency was indeed demonstrated but with a phase relation inverted with respect to TCV. In the ASDEX Upgrade experiments ELMs were found to be triggered with highest probability when the plasma moves down towards the X-point (lower single null configuration was used in these experiments). The experiments in ASDEX Upgrade demonstrated the potential to increase the ELM frequency and, accordingly, reduce the ELM energy losses up to a factor of 1.8 that of the initial or uncontrolled ELMs. In addition, it was also demonstrated that the ELM frequency could be reduced under the initial or uncontrolled ELM frequency by about 25 %. Due to hardware limitations it was not possible to increase further the frequency of triggered ELMs, as the effective plasma movement at higher frequencies was very low for the limits in voltage that could be applied to the control system. It was also found that full synchronization of the triggering of ELMs with the driving plasma movement was only achieved if the wobbling amplitude was maintained above a given threshold. For amplitudes near, but under, this threshold some enhancement of the ELM frequency was achieved (but not up to that of the driving perturbation), while for lower amplitudes no effect on ELM frequency was detected. A reduced edge current was found when moving the plasma against the X-point (and vice-versa) as in the TCV experiments but, in contradiction to the simple picture derived from the TCV experiments, during this phase ELMs were triggered in ASDEX Upgrade. This could be an indication that the mechanisms leading to the triggering of type-III ELMs (TCV) and type-I ELMs (ASDEX Upgrade) by the application of this control scheme are different, which would not be unexpected on the basis of the physics picture for ELMs described in section 2.
Detailed analysis of the quasi-equilibrium plasma evolution in the real configuration, taking into account the large conducting in-vessel structures in the ASDEX Upgrade device, showed that the edge magnetic flux surfaces are deformed with sizeable changes to their squareness which are sufficient to alter the stability of medium-n edge kink-ballooning modes [111].

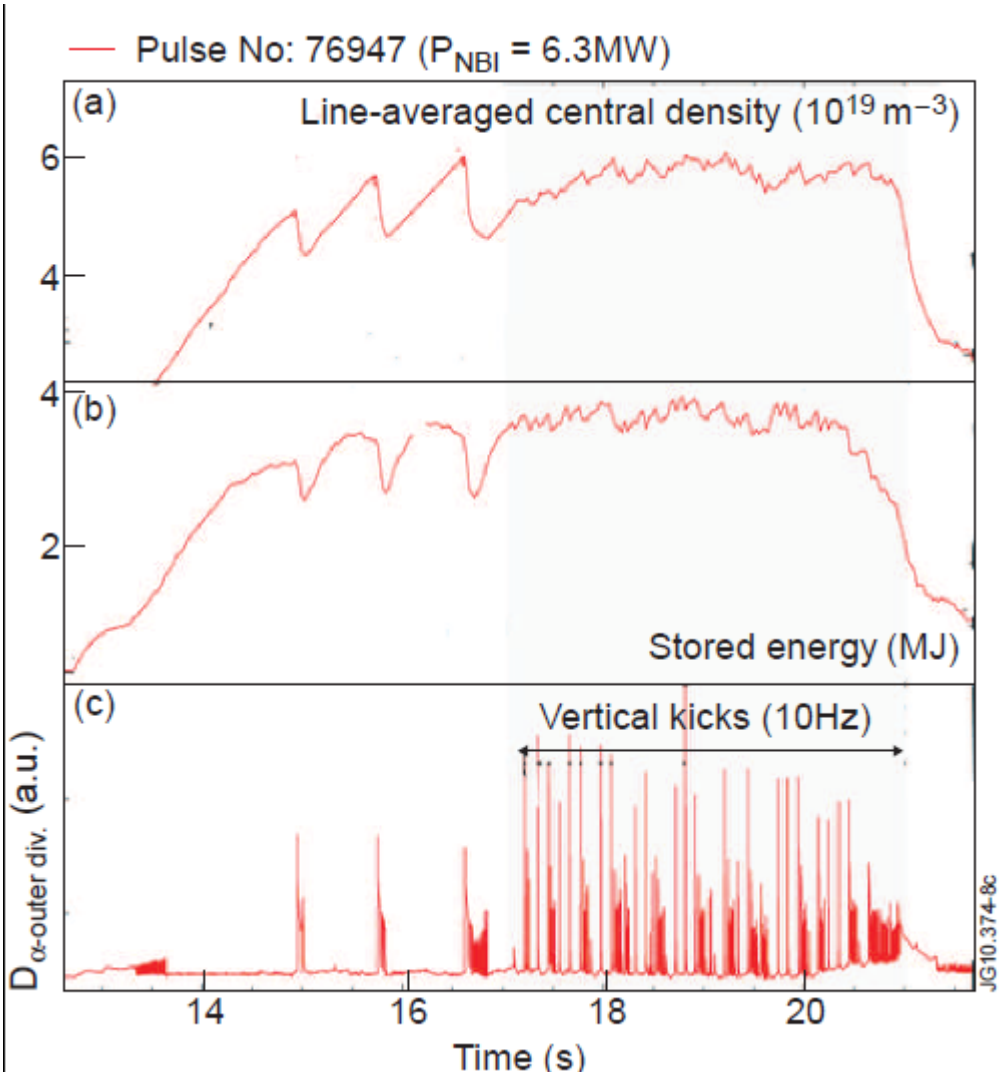

Figure 13: Application of „kicks" for the mitigation of very low frequency compound ELMs spontaneously occurring in a low δ plasma configuration with an applied heating power marginal above P_{HL}[19.81].

Applications of this technique for ELM control have also been reported for NSTX and Alcator C-mod [10]. However, the most extensive study to date has been performed at JET where the technique has matured to a level of reliability which allows its routine use as a control tool, for example, to prevent the occurrence of a long ELM-free periods ending in a compound ELM and a return to a type-III ELMy H-mode when accessing the H-mode at low power levels compared to the H mode threshold, as shown in figure 13 [19, 81]. At JET, fast vertical plasma movements ('vertical kicks') caused by perturbations injected through the vertical plasma position feedback loop are used to trigger type-I ELMs. Type-I ELMs can be triggered in ELM-free/type-I ELMy H-modes by vertical kicks and, as also found in ASDEX Upgrade, ELMs are triggered during the downwards motion of the plasma towards the X-point. At JET, the vertical movement of the plasma causes a larger deformation of the plasma shape than in other tokamaks due to the X-point being dominantly created by in-vessel divertor coils located close to the plasma. Thus the plasma column shrinks appreciable in the vertical direction when the plasma moves downwards with most of the decrease in height coming from the upper half of the plasma and very little change on the lower half, where the X-point is located. A threshold in plasma displacement/velocity needs to be exceed to trigger ELMs at the driving frequency of the kicks and, in conditions in which these threshold are

exceeded, a frequency enhancement of about 6 relative to the natural or uncontrolled ELM frequency (~10 Hz in these experiments) has been achieved. This maximum value of 60 Hz is due to hardware limitations and not limited by plasma related effects.
A strong reduction of the ELM size is observed with increasing trigger frequency by kicks. In general, no significant differences are found for triggered and spontaneous ELMs at the same frequency with respect to plasma energy loss, ELM affected plasma region, divertor power deposition and filamentary structure. In particular, ELM mitigation by fast plasma movement showed very similar behaviour than ELM mitigation by magnetic perturbations. In direct comparison discharges, the ELM frequency increase by both methods showed a similar reduction of pedestal pressure mainly due to density reduction (pump-out) and a moderate loss of plasma energy for plasmas with input powers well above the H-mode threshold. For powers near the H-mode threshold, on the contrary, ELM control by vertical kicks leads to an improvement of the plasma confinement [19, 81] which is opposite to the behaviour found with edge magnetic field perturbations [112] at JET. Recent calculations, applying a linear model for the modifications on the plasma and poloidal field coils during vertical kicks, showed a sharp variation in loop voltage during the kick cycle which induces strong edge current densities thus causing the edge plasma to become unstable to peeling modes [113].

Application of vertical plasma movements to control ELM in ITER
Beyond the general outstanding issues associated with ELM control by ELM pacing already discussed in the section on pellet pacing, this ELM control scheme has some aspects that are particularly attractive for application in ITER: a) it does not involve any resonant effects and thus can be applied to all phases of the discharge, b) it is compatible with a range of type-I ELMy H-mode operation conditions, c) it does not require an increase of the particle throughput beyond that needed to compensate the particle outflux caused by the controlled ELMs and d) it leads to an improvement of the plasma confinement when applied at low powers above the H-mode threshold for which sustainment of the type-I ELMy H-mode is marginal [19, 81], conditions which are very relevant for H-mode operation in ITER.
In the absence of a definitive physics criterion to evaluate the requirements for ITER, the required movement (peak-to-peak) of the plasma current centroid required triggering type-I ELMs in present experiments has been evaluated [10]. On the basis of these results, the guidance for the required plasma displacement in ITER to trigger ELMs by this method is in the range of 0.06 - 0.09 m. It is important to note that in this simple criterion the velocity of the plasma is not included. This is an important parameter in order to evaluate induced currents in the edge plasma and in the conducting structures surrounding the plasma and could modify the requirements derived from the application of the guidance criterion to ITER described above. The use of the ITER vertical stability in-vessel coils to cause repetitive plasma displacements to trigger ELMs has been simulated with the PET linear model [114]. A similar scheme to that in ASDEX Upgrade has been applied which takes into account the specifications of these coils and of their power supplies, presently designed for vertical stability control [10]. Vertical plasma movements for representative plasma conditions corresponding to a 15 MA Q_{DT} = 10 plasma with values of $l_i(3)$ = 0.7 and β_p = 0.65 have been modelled (the lay-out of the coils and the plasma is shown in Figure 14). The conducting structures, in 2-D approximation, considered for these studies include an axisymmetric model for the vacuum vessel, blanket support and divertor inboard rail and the proper specifications for the power supplies and coil cooling requirements [10] but no noise in the diagnostics of the plasma vertical displacement was included. The result of these studies is shown in Figure 15.

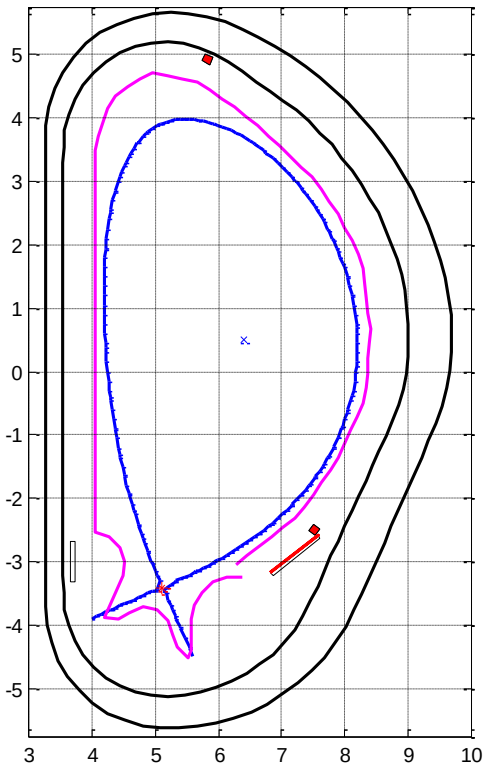

Figure 14: ITER plasma separatrix for modelled plasma 15 MA ($l_i(3) = 0.7$, $\beta_p = 0.65$), toroidally continuous conducting structures modelled and vertical stability in-vessel coils.

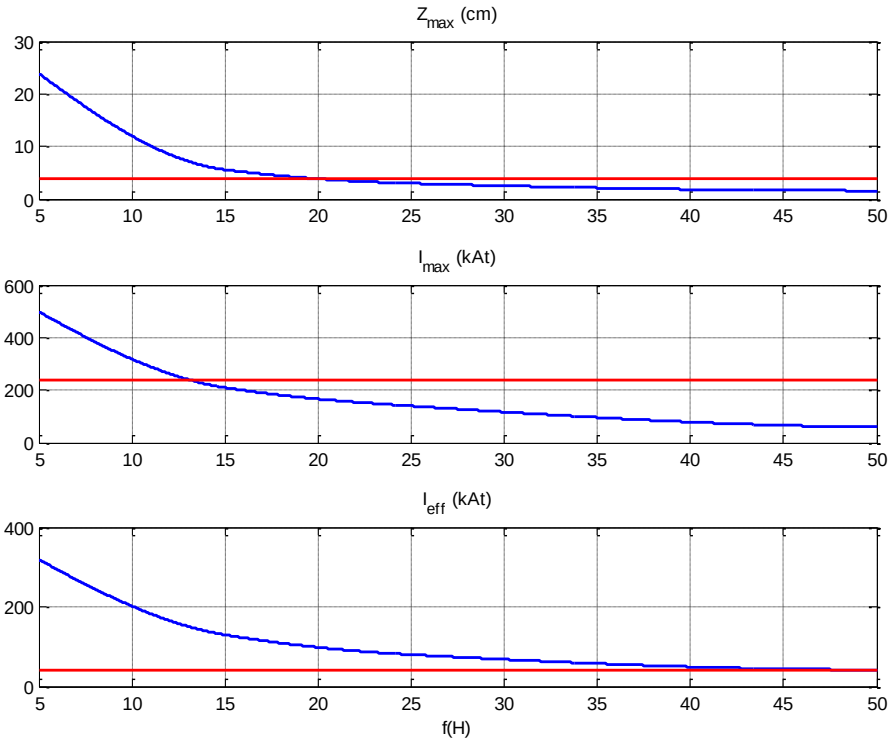

Figure 15: (From to bottom) The blue lines show the dependence of the maximum value of the plasma displacement peak-to-peak, maximum magnitude of the instantaneous current in the vertical stability coils and effective current in the vertical stability coils versus the frequency of the oscillations. The read lines indicate 4 cm peak-to-peak displacement (which is the maximum "natural" oscillation of the ITER plasmas caused by the plasma control system in which noise of RMS value of 0.6 m/s and 1 kHz bandwidth is consider for the control dZ/dt

measurement), the maximum current limit in the vertical stability coils of 240 kAt and limit of the effective current of 40 kAt, which is determined by the removal of the ohmic heating by the cooling circuit [10].

These simulations indicate that for the required frequencies of 30-60 Hz, the maximum achievable peak-to-peak displacement of the vertical position in ITER is in the range of 2-3 cm (0.3-0.5% of the plasma major radius), i.e., a factor of 3-5 times smaller than the guideline criterion deduced from direct scaling with size from present experimental results. Adding more realistic assumptions regarding noise may further reduce this value. Triggering of ELMs by such low value of the oscillation amplitude, which is comparable with the level of plasma vertical oscillations due to the noise expected in *dZ*/*dt* diagnostics, seems unlikely on the basis of evidence that the noise in *dZ*/*dt* diagnostics does not trigger ELMs in present tokamaks. Moreover, the effective value of current in the coils required for the 2-3 cm oscillations is at or beyond the design limit of the effective current (40 kAt). This will further limit the operation of the vertical stability control with in-vessel coils in case of large scale disturbances (e.g. minor VDEs) and noise in *dZ*/*dt* diagnostics. Larger plasma vertical shifts are achievable at lower frequencies (~ 12 cm peak to peak at 10 Hz) but the effective value of the current in the coils exceeds the design value of the system by a factor of 5 and this would lead to an intolerable overheating of the coils.

The analysis above shows that the potential for the application of this technique for ELM control in ITER for 15MA Q_{DT} = 10 plasmas with the design specifications of the coils and power supplies for vertical stability control is very low. It is also important to note that even if it were possible to upgrade the in-vessel vertical stability coil system for this purpose, if oscillations in the range of 6-9 cm are required to trigger ELMs, the vertically displaced and moving plasma may not be controllable by the ex-vessel vertical stability control system in ITER (which uses superconducting coils). Thus, any malfunction of the in-vessel vertical stability control, while performing the necessary oscillations for ELM control, would result in a full plasma energy VDE, which is highly undesirable for ITER at 15 MA. For lower plasma current scenarios or H-mode phases at lower currents in the 15 MA Q_{DT} = 10 scenario, this scheme may have more potential for application (at least for some phases of the discharge) although a precise evaluation has not yet been performed. Further quantification of this potential for lower current H-mode application requires a more solid physics basis for the mechanism leading to the triggering of ELMs with this technique.

7. Edge current drive and/or heating

Localized edge heating and current drive at the plasma edge could affect ELM behavior. From the peeling-ballooning stability model of edge stability described in section 2, it can be expected that the local deposition of heating and induction of currents in the pedestal region may affect the stability of the edge plasma and thus the ELMs. In some cases, this may lead to the triggering of ELMs at higher frequencies but not of smaller size as such and thus may not be a suitable scheme for ELM control. For instance, if the increase of ELM frequency is linear with the increase of additional heating power, no decrease in ELM energy loss is expected given the relation between ELM energy loss, ELM frequency and additional heating power described in section 2. The actuators for this control scheme are based on heating and current drive systems which are able to drive sufficient current or deposit sufficient heating power localized to the plasma edge. In principle, this control approach is rather straightforward, although it has obvious technical difficulties related to edge power/deposition and current drive, but no clear demonstration of a significant effectiveness on ELM control has been achieved so far.

Status of investigations

Attempts to control ELMs using modulated edge electron cyclotron heating and current drive have been reported for ASDEX Upgrade [115], JT-60U [14] and TCV [116] and modifications to the edge pedestal behaviour have been seen with LHCD in Alcator C-mod [117]. At ASDEX Upgrade, synchronization of the ELM frequency with modulated edge ECRH heating has been observed, albeit both with current drive driving currents of a similar value to the bootstrap current and with pure ECRH heating. ELM frequency locking to the ECRH modulation frequency was observed for an ELM frequency close to that expected without triggering and even when the ECRH modulation frequency was lower than the natural ELM frequency. It is thus thought likely that the main influence of the ECRH in this case was to modify the edge pressure profile rather than to directly drive current. In JT-60U the effects on the increase of the ELM frequency with the application of a constant ECRH power are significantly larger than those expected from the total increase of the edge plasma power flux and a decrease of the ELM energy loss of ~ 30% could be achieved. From a comparison of the expected edge current drive with the estimated bootstrap current, it seems unlikely that the observed effects are associated with any direct edge current drive. The most likely mechanism behind this behaviour is that local changes in the edge gradients are induced by the localised edge power deposition that in turn affects edge stability. Recent attempts at TCV applying the real time control system for ECRH [118] demonstrated ELM frequency control by power modulation. The same ELM frequency was found for modulated and steady state injection of power in the central region for the same average heating power level. However, when the same ECRH power level is deposited within a narrow deposition profile closer to the edge, f_{ELM} increased by a factor 1.5 – 2 even if it is not clear that a large amount of power was actually deposited within the pedestal region [118].

Application of edge heating and current drive for ELM control in ITER

The viability of this technique for ELM control in the 15 MA Q_{DT} = 10 scenario is very limited [10]. Firstly, the capability of the ECRH launcher to inject power at the edge is limited to 7 MW (for 20 MW of total power through the upper launcher) as shown in Figure 16 [11]. This is expected to drive a current of about 35% [11] of the pedestal current and it is unknown if such a level of edge current will modify ELMs at all and/or it will reduce the energy lost per ELM. Secondly, beyond design limitations of the launcher that could be re-optimised, the deposition of large amounts of ECRH power at the plasma edge involves serious risk of high power fluxes reaching "unexpected" in-vessel components in ITER due to imperfect absorption of the power at the edge. Finally, the power deposited at the edge will not contribute to central plasma heating (and hence to the increase of the fusion rate) and will, thus, lead to a decrease of the fusion gain. In addition, the use of ECRH for edge power deposition and ELM control in ITER implies that an additional launcher is required for this task, as the main purpose of the ECRH upper launcher (which aims at the edge plasma) is NTM control. It is expected that NTM control by ECCD will be needed during high Q_{DT} operation in ITER and this control will be simultaneous to that of ELM control. For all these reasons, the potential of this technique as an ELM control scheme in ITER appears to be very uncertain. The foreseen strategy with regards to the application of this ELM control technique to ITER operation is that first a demonstration of the effect would be attempted with the existing edge heating capabilities in the ITER Baseline and, if successful, this requirement could be considered for future power upgrades in ITER should it prove necessary.

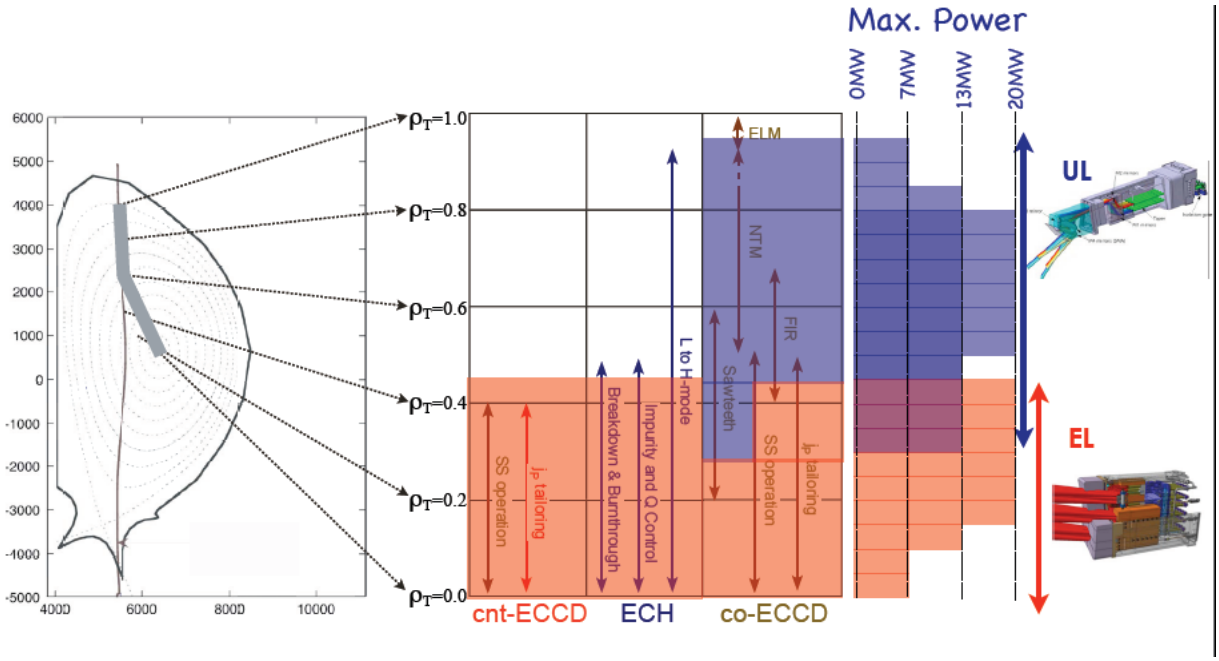

Figure 16: Capabilities for heating and current drive of the ITER Baseline ECRH system (Equatorial Launcher and Upper Launcher) for a total injected power of 20 MW versus for the various positions in the ITER plasma cross section [11].

8. Conclusion

Control of type-I ELMs is required for the operation of ITER in high power high confinement regimes envisaged for demonstration of high fusion gain in order to avoid unacceptable erosion and possible damage of the plasma facing components. ITER operation in the high Q regimes will take place in plasmas at low collisionality but high density (normalized to the Greenwald limit), a combination which cannot be fulfilled in present day tokamaks. This introduces considerable uncertainties regarding the extrapolation of ELM control techniques which are being developed intensely in present experiments. Two approaches are being followed to achieve the required level of ELM control in ITER: modification of the pedestal plasma so that it is not unstable to the instabilities causing the ELM (ELM suppression) or the triggering of the ELM instability at a sufficiently high frequency so that the ensuing ELM energy losses are controlled (ELM pacing). At present, several schemes have been demonstrated along these two lines but none to the level which will be eventually required in ITER when all scenario requirements are taken into account.

The remaining uncertainties in the scaling from present day machines to ITER are mostly due to the lack of sufficient knowledge of the underlying physics processes that lead to ELM suppression or the requirements and ultimate limits for ELM pacing. In view of the seriousness of the ELM control problem and the existing uncertainties in the application of existing schemes in ITER, the two most promising options for ELM suppression and control are being considered for implementation in ITER. The design of the ITER in-vessel edge magnetic perturbation coils system has already been developed to a very detailed stage. Its maximum current capability has been determined on the basis of empirical guidance from experiments and is able to provide levels of magnetic field perturbation at which large effects, when not suppression, is observed in most experiments. In addition, the system is maintained as flexible as possible (every coil is power independently) so that it can accommodate variations in the requirements for ELM suppression and its performance is maintained robustly in the event of a limited number of coils failing. Regarding ELM control by pacing the most promising technique from existing experiments is being considered, namely pellet pacing. The requirements for ELM pellet pacing in ITER, evaluated on the basis of existing experimental results, are taken into account in the design of the pellet launchers but, if

experience in ITER would prove that they are not appropriate or optimum for this role, their design could be modified without major integration problems with the rest of the device, as they are external systems to the torus.
No further dedicated systems for ELM control are being considered for ITER [10]. Instead the potential use of systems which will be installed in ITER for other purposes (in-vessel vertical stability coils, ECRH launchers, etc,) for ELM control within their original specifications is being explored. Unavoidably this implies that their use may not be suitable for ELM control in the reference burning phase of high Q scenarios but they may be applicable to lower current plasmas or to low current phases of such scenarios, if this is found to be advantageous. This consideration also applies to the small ELM/no ELM regimes which have been identified in present experiments.
Further experimental, theoretical and modeling R&D is required both to provide a sound physics basis to the ELM control schemes considered for ITER as well as for their practical application and integration with the other ITER plasma scenario requirements. This includes not only the high Q burning plasma scenarios but also the plasmas foreseen for the initial non-active phase of ITER operation, in which the ITER ELM control schemes will have to be tested and its application developed.

Disclaimer: The views and opinions expressed herein do not necessarily reflect those of the European Commission or those of the ITER Organization.

References

[1] H. Zohm, Plasma Phys. Control. Fusion **38** (1996) 105.
[2] W. Suttrop, Plasma Phys. Control. Fusion **42** (2000) A1.
[3] T. Eich et al., Phys. Rev. Lett. **91** (2003) 5003.
[4] J. Pamela et al., Nuclear Fusion **42** (2002) 1540.
[5] A. Loarte et al., Proc. 20th Int. Conf. on Fusion Energy, Chengdu (China), (Vienna, IAEA) IT/P1-14, 2006.
[6] A. Loarte et al., Plasma Phys. Control. Fusion **45** (2003) 1549.
[7] Progress in the ITER Physics Basis **47** (2007) S1.
[8] Loarte et al., Proc. 23rd Int. Conf. on Fusion Energy, Daejeon (Korea), (Vienna, IAEA) IT/I1-5, 2010.
[9] R. Dejarnac et al., J. Nucl. Mater. **390-391** (2009) 818.
[10] "Plan for ELM Mitigation in ITER", ITER Technical Report.
[11] T. Eich, 19th Int. Conf. on Plasma Surface Interaction, San Diego, O-6, 2010.
[12] "Evaluation of ELM control needs and options in ITER", Fusion for Energy Technical Report.
[13] P. B. Snyder et al., Nuclear Fusion **44** (2004) 320.
[14] N. Oyama, Journal of Physics: Conference Series 123 (2008) 012002.
[15] A. Burckhart et al., Plasma Phys. Control. Fusion **52** (2010) 105010.
[16] H.R. Wilson and S.C. Cowley, Phys. Rev. Lett. **92** (2004) 175006.
[17] A. Loarte et al., Proc. 18th Int. Conf. on Fusion Energy 2000, Sorrento, IAEA-CN-77 ITERP/11(R), 2000.
[18] A.Herrmann, Plasma Phys. Control. Fusion **44** (2002**)** 883.
[19] E. De La Luna et al., Proc. 23rd Int. Conf. on Fusion Energy, Daejon (Korea Rep.), (Vienna, IAEA) EXC/8-4, 2010; EFDA-JET-CP(10)08/37.
[20] N. Oyama et al., Plasma Phys. Control. Fusion **48** (2006) A171.
[21] N. Oyama, ITPA "Pedestal & Edge Physics" meeting, Naka (Japan), April 2010.
[22] J.L. Terry et al., Nuclear Fusion **45** (2005) 1321.
[23] K. Kamiya, N. Oyama, T. Ido, M. Bakhtiari, JFT-2M Group, Phys. Plasmas **13** (2006) 032507.

[24] J. Wesson, Tokamaks, second edition, Clarendon Press, Oxford (1997) chapter 4.6 & 4.9.
[25] Y. Kamada et al., Plasma Phys. Control. Fusion **44** (2002) A279.
[26] N. Oyama et al., Plasma Phys. Control. Fusion **49** (2007) 249.
[27] J. Stober et al., Nucl. Fusion **45** (2005) 1213.
[28] G. Saibene et al., Nucl. Fusion **45** (2005) 297.
[29] W. Suttrop et al., Plasma Phys. Control. Fusion **39** (1997) 2051.
[30] J. Rapp et al., Nucl. Fusion **49** (2009) 095012.
[31] N. Asakura et al., Nucl. Fusion **49** 115010 (2009).
[32] I. Nunes et al., Proc. 34th EPS Conf. on Plasma Phys., Vol **31F** P-5.137 (2007).
[33] R. Maingi et al., Nucl. Fusion **45** (2005) 264.
[34] R. Maingi et al., Phys. Plasmas **13** (2006) 092510.
[35] K.H. Burrell et al., Plasma Phys. Control. Fusion **44** (2002) A253.
[36] W. Suttrop et al., Plasma Phys. Control. Fusion **45** (1997) 1399.
[37] Y. Sakamoto et al., Plasma Phys. Control. Fusion **46** (1997) A299.
[38] W. Suttrop et al., Nucl. Fusion **45** (2005) 721.
[39] A. Garofalo, ITPA "Pedestal & Edge Physics" meeting, Naka (Japan), April 2010.
[40] K. Burrell et al., Nucl. Fusion **49** (2009) 085024.
[41] W.P. West et al., Nucl. Fusion **45** (2005) 1708.
[42] P. Snyder, et al., Nucl. Fusion **47** (2007) 961.
[43] P. B. Snyder, et al., Nucl. Fusion **41** (2011) 103016.
[44] J. Rapp et al., Nucl. Fusion **44** (2004) 312.
[45] P. Monier-Garbet et al., Nucl. Fusion **45** (2005) 1404.
[46] A. Kallenbach et al., J. Nucl. Mater. **337–339 (**2005) 732.
[47] J. Schweinzer et al., Nucl. Fusion **51** (2011) 113003.
[48] P.T. Lang et al., Nucl. Fusion **45** (2005) 502.
[49] A. Grosman et al., J. Nucl. Mater. **313-316** (2003) 1314.
[50] A.B. Rechester and M.N. Rosenbluth, Phys. Rev. Lett. **40** (1978) 38.
[51] T.E. Evans, 13thWorkshop H-mode Physics, Oxford, O2, 2011.
[52] W. Suttrop et al., Phys. Rev. Lett. **106** (2011) 225004.
[53] T.E. Evans et al., Nucl. Fusion **45** (2005) 595.
[54] Ph. Ghendrih et al., Nucl. Fusion **41** (2001)1401.
[55] O.Schmitz et al., Nucl. Fusion **48** (2008) 024009.
[56] N. Ohyabu et al., Nucl. Fusion **27** (1987) 2178.
[57] H. Tamai et al., J. Nucl. Mater. **220-222** (1994) 365.
[58] S.J. Fielding et al., Proc. 28th EPS Conference on Controlled Fusion and Plasma Physics, ECA, 25A (2001) 1825.
[59] T.E. Evans et al., Phys. Rev. Lett. **92** (2004) 235003.
[60] T. H. Osborne et al., Proc. 32nd EPS Conference on Controlled Fusion and Plasma Physics, Tarragona , P4.012, 2005.
[61] T.E. Evans et al., Nature Physics **2** (2006) 419.
[62] T.E. Evans et al., Nucl. Fusion **48** (2008) 024002.
[63] M.E. Fenstermacher et al., Phys. Plasmas 15 (2008) 056122.
[64] Y. Liang et al., Plasma Phys Control Fusion **49** (2007) B581.
[65] Y. Liang et al., Plasma Fusion Research **5** (2010) S2018.
[66] J.M. Canik et al., Nucl. Fusion **50** (2010) 034012.
[67] A. Kirk et al., 19th Int. Conf. on Plasma Surface Interaction, San Diego, P1-40;
J. Nucl. Mater., in press (2011) doi:10.1016/j.jnucmat.2011.01.012.
[68] P.T. Lang, et al., Nucl. Fusion **52** (2012) 023017.

[69] H. Strauss et al., Nucl. Fusion **49** (2009) 055025.
[70] M. Becoulet et al., Nucl. Fusion **49** (2009) 085011.

[71] M. Becoulet et al., Proc. 37th EPS Conference on Controlled Fusion and Plasma Physics, Dublin, P4-105, 2010.
[72] D. Reiser et al., Phys. Plasmas **16** (2009) 042317.
[73] E. Nardon et al. A. Kirk et al., 19th Int. Conf. on Plasma Surface Interaction, San Diego, P1-43.
[74] M.W. Jakubowskiet al., Nucl. Fusion 49 (2009) 095013.
[75] Q. Yu and S. Günter, Nucl. Fusion **49** (2009) 062001.
[76] C. Neumeyer et al., Fus. Sci. Tech. **60** (2011) 95.
[77] D. Orlov, et al., Fusion Sci. Tech., in press.
[78] O. Schmitz, et al., Jour. Nuc. Mat. **415** (2011) S886-S893.
[79] O. Schmitz, et al., Plasma Phys. Control. Fusion **50** (2008) 124029.
[80] M.Schaffer, Private communication, 2009.
[81] E. De La Luna et al., 51st Annual Meeting of the Division of Plasma Physics,Atlanta (U.S.A.), 2009.
[82] T. E. Evans, ITPA "Transport & Confinement" meeting, Naka (Japan), April 2010.
[83] M. Fenstermacher et al., Proc. 23rd Int. Conf. on Fusion Energy 2010, Daejeon, ITR/P1-30, 2010.
[84] M. Fenstermacher et al., ITPA Pedestal Meeting, York, UK, 2001.
[85] K.H. Burrell et al., Plasma Phys. Control. Fusion **47** (2005) B37.
[86] J.W. Ahn, et al., Nucl. Fusion **50** (2010) 045010.
[87] H. Frerichs et al., Nucl. Fusion **50** (2010) 034004.
[88] J.W. Ahn, et al., Proc. 38th EPS Conference on Controlled Fusion and Plasma Physics, Strassbourg, P1.060, 2011.
[89] T. Petrie, et al., J. Nucl. Mat. **415** (2011) S906-S909.
[90] P.T. Lang et al., Nucl. Fusion 44 (2004) 665.
[91] H. Urano et al., Plasma Phys. Control. Fusion **46** (2004) A315.
[92] F. Romanelli et al., Nucl. Fusion 49 (2009) 104006.
[93] B. Alper et al., Proc. 29th EPS Conference on Controlled Fusion and Plasma Physics, Montreux, P1.025, 2002
[94] L.R. Baylor et al., Proc. 37th EPS Conference on Controlled Fusion and Plasma Physics, Dublin, P2.117, 2010.
[95] L.R. Baylor, et al., Proc. 39th EPS Conference on Controlled Fusion and Plasma Physics, Stockholm, O4.113, 2012.
[96] P.T. Lang et al., Proc. 38th EPS Conference on Controlled Fusion and Plasma Physics, Strasbourg, O3.112, 2011.
[97] P.T. Lang et al., Nucl. Fusion **48** (2008) 095007.
[98] G.T.A. Huysmans et al., Plasma Phys. Control. Fusion **51** (2009) 124012.
[99] G.T.A. Huysmans, Proc. 37th EPS Conference on Controlled Fusion and Plasma Physics, Dublin, P4.132, 2010.
[100] G. Kocsis et al., Proc. 37th EPS Conference on Controlled Fusion and Plasma Physics, Dublin, P4.136, 2010.
[101] R.P. Wenninger et al., Plasma Phys. Control. Fusion **53** (2011) 105002.
[102] T. Eich, T., J. Nucl. Mat. **415** (2011) S856-S859.
[103] A. Loarte, et al., Plasma Phys. Control. Fusion **44** (2002) 1815.
[104] K. Gál et al., Proc. 22nd IAEA Fusion Energy Conference, Geneva, IAEA-CN-165/ TH/P4-5, 2008.
[105] S. Futatani, et al., Proc. 13th International Workshop on H-mode Physics and Transport Barriers, Oxford, UK, 2011.
[106] P.T. Lang, et al., Nucl. Fusion **51** (2011) 033010.
[107] A. Kukushkin, et al., Proc. 36th EPS Conference on Controlled Fusion and Plasma Physics, Sofia, P4. 167, 2009.

[108] A. Polevoi, et al., Proc. 38th EPS Conference on Controlled Fusion and Plasma Physics, Strassbourg, P4.109, 2011.
[109] A.W. Degeling et al., Plasma Phys. Control. Fusion **45** (2003) 1637.
[110] P T Lang et al., Plasma Phys. Control. Fusion **46** (2004) L31.
[111] S.H. Kim et al., Proc. 32nd EPS Conference on Controlled Fusion and Plasma Physics, Tarragona, P5.014, 2005.
[112] G. Saibene, ITPA Edge and Pedestal Group & Confinement Meeting, Naka (Japan), April 2010.
[113] F. Koechl et al., 13th Workshop H-mode Physics, Oxford, P2.21, 2011.
[114] S.A. Galkin Nucl. Fusion **37** (1997) 1455.
[115] L.D. Horton et al., Plasma Phys. Control. Fusion **46** (2004) B511.
[116] F. Felici, EPFL thesis no. 5203, Lausanne, Switzerland, 2011.
[117] J. Hughes, et al., 12th Workshop H-mode Physics, Pinceton, 2009.
[118] F. Felici et al., Nucl. Fusion **51** (2011) 083052.